



Characterization of a novel JNK (c-Jun N-terminal kinase) inhibitory peptide

Kevin R. W. NGOEI*, Bruno CATIMEL†, Nicole CHURCH†, Daisy S. LIO*, Con DOGOVSKI*, Matthew A. PERUGINI*, Paul M. WATT‡, Heung-Chin CHENG*, Dominic C. H. NG* and Marie A. BOGOYEVITCH*¹

*Department of Biochemistry and Molecular Biology, Bio21 Molecular Science and Biotechnology Institute, University of Melbourne, Parkville, Victoria 3010, Australia,

†Ludwig Institute for Cancer Research, Parkville, Victoria 3010, Australia, and ‡Phylogica Ltd, Subiaco, Western Australia 6008, Australia

An improved understanding of the roles of protein kinases in intracellular signalling and disease progression has driven significant advances in protein kinase inhibitor discovery. Peptide inhibitors that target the kinase protein substrate-binding site have continued to attract attention. In the present paper, we describe a novel JNK (c-Jun N-terminal kinase) inhibitory peptide PYC71N, which inhibits JNK activity *in vitro* towards a range of recombinant protein substrates including the transcription factors c-Jun, ATF2 (activating transcription factor 2) and Elk1, and the microtubule regulatory protein DCX (doublecortin). Analysis of cell culture studies confirmed the actions of a cell-permeable version of PYC71 to inhibit c-Jun phosphorylation during acute hyperosmotic stress. The analysis of the *in vitro* data for the kinetics of this inhibition indicated a substrate–inhibitor complex-mediated inhibition of JNK by PYC71N. Alanine-scanning replacement studies revealed the importance of two residues (PYC71N Phe⁹ or Phe¹¹ within an FXF motif) for

JNK inhibition. The importance of these residues was confirmed through interaction studies showing that each change decreased interaction of the peptide with c-Jun. Furthermore, PYC71N interacted with both non-phosphorylated (inactive) JNK1 and the substrate c-Jun, but did not recognize active JNK1. In contrast, a previously characterized JNK-inhibitory peptide TIJIP [truncated inhibitory region of JIP (JNK-interacting protein)], showed stronger interaction with active JNK1. Competition binding analysis confirmed that PYC71N inhibited the interaction of c-Jun with JNK1. Taken together, the results of the present study define novel properties of the PYC71N peptide as well as differences from the characterized TIJIP, and highlight the value of these peptides to probe the biochemistry of JNK-mediated substrate interactions and phosphorylation.

Key words: binding analysis, c-Jun N-terminal kinase, kinetic analysis, peptide inhibitor, substrate–inhibitor complex.

INTRODUCTION

The JNKs (c-Jun N-terminal kinases) are a group of serine/threonine protein kinases within the larger MAPK (mitogen-activated protein kinase) family. First described as a group of stress-activated protein kinases [1,2], JNKs have continued to attract attention owing to their activation in response to a range of stress and cytokines, as well as their roles in the regulation of cell death and survival [3]. Further interest has been stimulated by the implication, largely through gene-knockout studies, of JNKs as key targets for therapeutic intervention in the treatment of a range of pathologies including diabetes [4], stroke [5] and liver disease [6]. This has further stimulated efforts to discover new JNK-inhibitory molecules.

The discovery process for JNK inhibitors has generally involved the screening of proprietary chemical libraries for inhibition of JNK activity *in vitro* (for a review see [7]). This approach has revealed ATP-competitive inhibitors of JNK such as SP600125 [8], AS601245 [9] and other small molecule inhibitors [10]. However, the identification of a small peptide derived from the JNK pathway scaffolding protein, JIP (JNK-interacting protein) 1 [11], has shown that ATP-non-competitive inhibitors are useful alternatives to the small molecule ATP-competitive inhibitors. Indeed, this minimal inhibitory peptide derived from JIP1 interacts with the substrate-docking site of JNK [12], and competes with protein substrates for binding to JNK. Although this provides interesting biochemical insights into the mechanisms

used by JNK to recruit its specific downstream substrate proteins, further use of cell-permeable versions of these peptides has generated considerable interest with the observed beneficial effects to improve neuronal survival following insult to the brain [13] and to improve symptoms in diabetes [14].

Despite these advances, new strategies may additionally discover novel classes of JNK-inhibitory molecules. Approaches directed towards preventing the interaction of JNK with the JIP-derived peptides have revealed the first examples of ATP-non-competitive small molecule inhibitors of JNK [15–18]. It has therefore been of further interest to explore whether other peptides might also inhibit JNK. These peptides could provide insights into the regulation of the actions of JNK, as well as guiding the design and/or screening of new JNK inhibitors. In the present paper, we report our characterization of a novel JNK-inhibitory peptide, identified originally during the screening of a biodiverse gene fragment library [19,20]. The 22 amino acid peptide (named PYC71), despite showing no sequence identity to the JIP-derived inhibitory peptide previously described [11], required the presence of two phenylalanine residues within an FXF motif of the N-terminal fragment for its inhibitory actions. Furthermore, the minimal inhibitory 13 amino acid peptide (PYC71N) could inhibit JNK activity towards different substrates, and showed kinetics of inhibition consistent with a model in which a peptide–substrate complex was the inhibitory species. In addition, binding analysis showed that PYC71N prevented the interaction of JNK with c-Jun. Thus the PYC71N peptide represents a novel tool

Abbreviations used: DCX, doublecortin; ERK, extracellular-signal-regulated kinase; GST, glutathione transferase; HBS, HEPES-buffered saline; JNK, c-Jun N-terminal kinase; JIP, JNK-interacting protein; MAPK, mitogen-activated protein kinase; MKK, MAPK kinase; R_{max}, maximum analyte binding capacity; RMSD, root mean square deviation; RU, response units; *Sf9*, *Spodoptera frugiperda* 9; SPR, surface plasmon resonance; TFE, trifluoroethanol; TIJIP, truncated inhibitory region of JIP.

¹ To whom correspondence should be addressed (email marieb@unimelb.edu.au).

to further explore JNK-mediated phosphorylation of its protein substrates.

MATERIALS AND METHODS

Bacterial expression and preparation of recombinant JNK substrate proteins

The JNK substrates [c-Jun(1–135), ATF2(19–96), Elk1(307–428) and DCX(1–362)] were prepared from *Escherichia coli* as GST (glutathione transferase)-fusion proteins. For interaction analyses by SPR (surface plasmon resonance; BIAcore), GST was removed by proteolytic cleavage using thrombin [Sigma; 50 units/ml, 22 °C, overnight with shaking, for GST–c-Jun(1–135), GST–ATF2(19–96) and GST–Elk1(307–428)].

Baculovirus expression vectors for JNK1 α 1, MKK (MAPK kinase) 4 and MKK7

Full-length *JNK1* cDNA containing a GST tag at the 5' position was subcloned into the XbaI and XhoI sites in a pBACPAK9 vector (Clontech) to create the plasmid pBACPAK9–GST–JNK1. In addition, full length but untagged MKK4 and MKK7 constructs were subcloned to create pBACPAK9–MKK4 and pBACPAK9–MKK7 plasmids. Each of these plasmids was individually co-transfected with BACPAK6 baculoviral DNA into *Sf9* (*Spodoptera frugiperda* 9) insect cells to generate recombinant JNK1 α 1, MKK4 and MKK7 baculoviruses, according to the manufacturer's protocol (Clontech). Western blotting was conducted using anti-JNK antibodies (BD Biosciences), anti-MKK4 or anti-MKK7 antibodies (Santa Cruz Biotechnology) to determine protein expression post-infection, and each recombinant baculovirus was subsequently enriched through plaque purification assays.

Purification of recombinant JNK1 α 1 (active and inactive) from *Sf9* insect cells

Cultures (1 litre) of *Sf9* cells (1×10^6 cells/ml) were infected with recombinant JNK1 α 1 baculovirus. For production of the active form of JNK1 α 1, the culture was co-infected with baculovirus encoding the upstream kinases MKK4 and MKK7. Each virus was used at a multiplicity of infection of ≥ 1.0 . After 3 days post-infection, cells were harvested by centrifugation (1000 *g* at 20 °C for 5 min) for further purification of JNK using standard GSH–Sepharose affinity followed by ion-exchange chromatography. The GST tag was removed by PreScission Protease (GE Healthcare; 40 units/ml, 4 °C, 4 h with shaking) cleavage prior to further use of the JNK1 α 1 protein in SPR (BIAcore) analyses.

Peptide sequences and synthesis

The sequences of peptides evaluated in our *in vitro* studies are shown in Table 1. PYC71 and PYC71N, its shorter N-terminal fragment, were synthesized by Peptide Technologies. The positive control JNK-inhibitory peptide TIJIP (truncated inhibitory region of JIP) [11], was synthesized by Proteomics International. For interaction analyses by SPR, PYC71 or PYC71N were resynthesized (Peptide Technologies) to include an N-terminal aminohexanoic acid-biotin-tag to allow immobilization to the BIAcore chip surface. For the evaluation of JNK inhibition in cells, the PYC71 peptide was synthesized as a C-terminal extension of the cell-permeable TAT sequence or as the retroinverso D-amino acid form by Auspep as described previously [20]. The TAT-conjugated TIJIP peptide was also synthesized by Auspep [20].

Table 1 Sequences of TIJIP, PYC71 and PYC71 peptide fragments

Peptide name	Peptide sequence	Peptide size (amino acid number)
TIJIP	RPKRPTLLNLF	11
PYC71	FFWRLNKIFYFIDSRVAAAILN	22
PYC71N	FFWRLNKIFYFID	13
PYC71M	RLNKIFYFIDSRV	13
PYC71C	YFIDSRVAAAILN	13

The purity of all peptides was determined to be >80% by HPLC and MS. To determine the residues critical for JNK inhibition, modified versions of the PYC71N peptide were made as indicated previously, with either N- or C-terminal truncation, or the substitution of residues Arg⁴, Leu⁵, Lys⁷ and Phe⁹ with either glycine, proline or phenylalanine to further evaluate the contributions by the amino acids at these specific positions. This additional series of peptides, each up to 13 amino acids in length, was synthesized by Mimotopes using multipin technology. All peptides were dissolved in DMSO at room temperature (20 °C) with brief vortexing and remained soluble under subsequent assay conditions. Peptide-mediated inhibition of JNK was subsequently examined by *in vitro* kinase assays.

CD spectroscopy

CD spectra of PYC71 and PYC71N (150 μ g/ml in 20 mM sodium acetate buffer, pH 5.0) were acquired using a Model 410SF CD Spectrometer (Aviv Biomedical) at 20 °C in a 1 mm Quartz cuvette from 190 to 240 nm with a 0.5 nm step size and 2.0 s average time. The spectra of peptides were also recorded in the presence of 30% TFE (trifluoroethanol) in 20 mM acetate buffer, pH 5.0. All spectra were fitted by non-linear regression analysis using the CDPro software package [21] employing the CONTINLL algorithm and either the SP22X, SP37A, SP29 or SMP56 databases, with the differences between the observed and model values expressed as RMSD (root mean square deviation) (Supplementary Table S1 at <http://www.BiochemJ.org/bj/434/bj4340399add.htm>). CD spectra of the recombinant JNK1 protein expressed in baculovirus were also obtained and consistent with a folded protein with α -helix and β -sheet characteristics.

Analytical ultracentrifugation

Sedimentation equilibrium experiments of PYC71 and PYC71N were conducted in an XLOI analytical ultracentrifuge (Beckman–Coulter) using a four-hole An60-Ti rotor against a buffer reference (20 mM sodium acetate buffer, pH 5.0) at 20 °C. Data were obtained at a rotor velocity of 50000 rev./min and a wavelength of 280 nm, using a step size of 0.001 cm and 10 averages until sedimentation equilibrium was attained (after 24 h). Sedimentation equilibrium profiles of the peptides were fitted to a single species model using SEDPHAT [22] with the differences between the observed and calculated values expressed as RMSD.

In vitro kinase assays

The activity of the JNK isoforms JNK1 α 1, JNK2 α 2 and JNK3 α 1, as well as the related MAPKs p38 α and ERK (extracellular-signal-regulated kinase) 2 (Upstate Cell Signalling Solutions/Millipore) towards recombinant GST-fusion proteins of different substrates [10 μ g; either the transcription factors: c-Jun(1–135), ATF2(19–96) or Elk1(307–428), or the microtubule regulatory protein DCX

(doublecortin), was examined at various PYC71 or PYC71N concentrations (10, 50 and 100 μM as indicated) in a kinase reaction buffer (20 mM Hepes, 20 mM 2-glycerophosphate, pH 7.6, supplemented with 20 mM MgCl_2 , 25 μM sodium orthovanadate and 100 μM dithiothreitol). After pre-incubation (5 min) of JNK with its protein substrate and peptide inhibitors, each kinase reaction was initiated by the addition of ATP (5 μM ATP and 1 μCi of $[\gamma\text{-}^{32}\text{P}]\text{ATP}$) followed by incubation for 20 min at 30°C. Phosphorylated proteins were separated by SDS/PAGE (12% gel), and ^{32}P incorporation was visualized using autoradiography and then quantitated by liquid scintillation counting. Additional control assays included the characterized JNK-inhibitory peptide TIJIP [11]. All assays were repeated on a minimum of three independent occasions and statistically significant differences in inhibition by the tested peptides were determined by Student's paired *t* test.

To assess the mechanisms of JNK inhibition by the PYC71N peptide, the concentrations of GST-c-Jun(1–135) and ATP were varied along with the concentration of PYC71N (0.8–8.1 μM , 0.26–5.3 μM and 10–40 μM respectively). Data were analysed in two ways. First, double-reciprocal plot $\{1/v [\text{min}/\text{pmol}] \text{ compared with } 1/[\text{GST-c-Jun}(1-135)] [\mu\text{M}^{-1}] \text{ or } 1/[\text{ATP}] [\mu\text{M}^{-1}]\}$ and linear regression analysis was performed. To further analyse the pattern of PYC71N-mediated JNK inhibition, data was replotted as reaction velocity (*v*) compared with PYC71N or TIJIP (μM) at 1, 2, 5 and 10 μg of GST-c-Jun(1–135).

Cell culture, treatment, lysis and immunoblotting

PC12 cells were maintained, exposed to hyperosmotic stress (0.5 M sorbitol, 30 min) and lysates were prepared as described previously [23]. Where indicated, cells were pre-exposed to either vehicle (DMSO), the ATP-competitive JNK inhibitor VIII (20 μM , Calbiochem, [10]), TAT-TIJIP (100 μM , [24]), or TAT-conjugated PYC71 peptides [20] for 30 min prior to hyperosmotic stress. Cell lysates were prepared in RIPA buffer [50 mM Tris/HCl, pH 7.3, 150 mM NaCl, 0.1 mM EDTA, 1% sodium deoxycholate, 1% (v/v) Triton X-100, 0.2% NaF and 100 μM sodium orthovanadate] supplemented with protease inhibitors. After 10 min on ice, cell debris was removed by centrifugation (14000 *g*, at 4°C for 10 min). Protein concentrations were then determined by Bradford assay. Protein lysates (20–50 μg) were resolved by SDS/PAGE (10% gel) transferred on to PVDF membranes and immunoblotted with antibodies recognizing phosphorylated c-Jun [p-c-Jun(Ser⁷³)], c-Jun, phosphorylated JNK (p-JNK) (Cell Signaling), JNK (BD Biosciences Australia) or α -tubulin (Sigma) [23,25]. Experiments were repeated on two independent occasions with comparable results.

SPR studies

The interaction studies between PYC71N peptides and JNK1 α 1 or its substrates were conducted using a BIAcore 2000 biosensor (BIAcore) [26]. Biotinylated-PYC71N or its alanine mutant versions were immobilized on to CM5 sensor chips via biotin-NeutrAvidin interaction. Prior to biosensor analysis, proteins were pre-diluted in 0.005% Tween 20 in HBS (Hepes-buffered saline; 10 mM Hepes, 3.4 mM EDTA and 0.150 mM NaCl, pH 7.4). Increasing protein concentrations were injected over the sensor surface at a flow rate of 10 $\mu\text{g}/\text{min}$ and binding profiles were recorded in real time as a sensorgram. All sensorgrams shown in the Results section have been corrected by subtraction of the corresponding signal obtained when the sample was injected over a NeutrAvidin control channel. Following completion of the

injection phase, the dissociation was monitored in HBS for 360 s at the same flow rate.

To define the mechanism of PYC71N inhibitory actions, competition-binding analysis was also conducted by assessing the binding of JNK1 towards immobilized GST-c-Jun(1–135) (immobilization level of 12 ng/mm²) in the presence or absence of bound PYC71N peptides at either 0.05 ng/mm² or 0.2 ng/mm². The baseline, indicating peptide stability, was confirmed prior to JNK1 injection at 3.3 μM . For simplicity of presentation of the results, the resulting binding curves of JNK1 interaction towards GST-c-Jun or GST-c-Jun/PYC71N were overlaid.

For kinetic analysis, the BIAevaluation software package (BIAcore version 4.1) was used for data processing and curve fitting. The apparent association and dissociation rate constants were calculated using global analysis with a 1:1 Langmuir interaction model that included mass transport parameters, as well as using Global Fitting algorithms [27].

The analysis of the regions of the sensorgrams where 1:1 Langmuir interactions appeared to be operative showed regions of the dissociation and association phases which were linear for plots of $\ln(R_0/R)$ compared against *t*. The dissociation rate constant (*k_d*) and association rate constant (*k_a*) obtained in this analysis were then used to calculate the equilibrium association (*K_A*) and dissociation constants (*K_D*). Global fitting algorithms incorporated a 1:1 model that included terms for mass transfer of analyte to the surface [analyte (A) bind to ligand (B)], as well as a heterogeneous ligand model that assumed that one analyte (A) binds independently to two ligand sites (B1 and B2). The goodness of fit between experimental data and fitted curves was estimated by χ^2 -squared analysis using the eqn (1)

$$\chi^2 = \frac{\sum_{i=1}^n (r_i - r_x)^2}{n - p} \quad (1)$$

where *r_i* is the fitted value at a given point, *r_x* is the experimental value at the same point, *n* is the number of data points and *p* is the number of degrees of freedom.

Comparison of the surface reactivity following different peptide immobilization was calculated as surface molar binding activity based on eqn (2) [28]:

Surface molar binding activity

$$= \frac{\text{JNK response unit} \times \text{peptide molecular mass}}{\text{peptide response unit} \times \text{JNK molecular mass}} \quad (2)$$

RESULTS

Identification and biophysical characterization of the JNK-inhibitory peptides PYC71 and PYC71N

A novel library of fragments amplified from the genomes of evolutionarily diverse bacteria and *Archaea* has been previously screened to identify API-inhibitory peptides [20]. We evaluated the identified peptides for inhibition of JNK-mediated phosphorylation of either full length c-Jun or the phosphorylation of the N-terminal transactivation domain (1–135) of c-Jun. This analysis revealed that, of five tested peptides [PYC34 (AYQSINSSPVLPEPNSQELSLHQHVTKS), PYC35 (AYQSIRSGGIESSSKRER), PYC36 (LQGRRRQGYSQSIKP), PYC38 (LQRRRQPGQPQGRWSGRALPAHR) and PYC71 (FFWRLNKIFYFIDSRVAAAILN)], the one denoted as PYC71 inhibited JNK1 activity under both assay conditions (Watt P., Barr R. and Bogoyevitch M., unpublished work). As shown in Table 1, PYC71 is a 22 amino acid peptide and so to

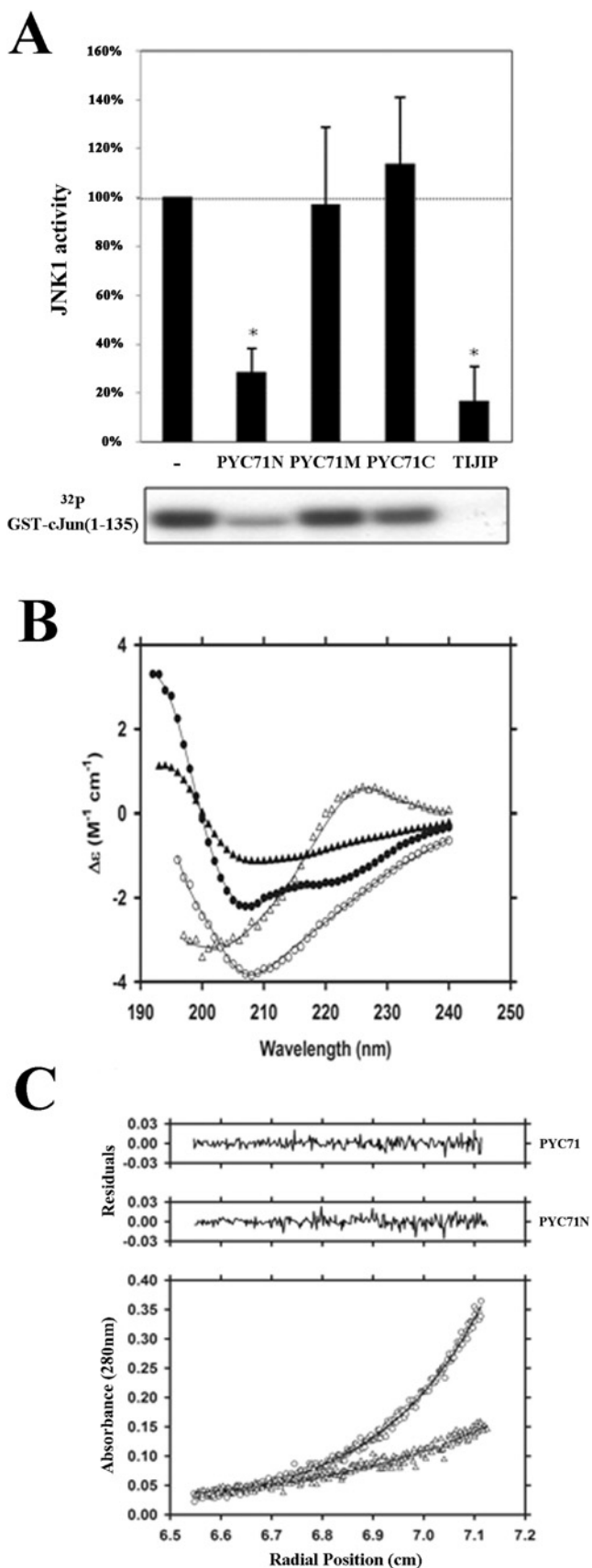


Figure 1 Characterization of the JNK inhibitory peptide PYC71 and its 13 amino acid N-terminal fragment PYC71N

identify the residues contributing to the JNK-inhibitory actions of PYC71, three peptides were synthesized that encompassed 13 amino acids of the N-terminal sequence (PYC71N), the middle sequence (PYC71M) or the C-terminal sequence (PYC71C). When each of these peptide variants was assayed at a final concentration of 100 μ M, only PYC71N retained JNK-inhibitory activity (Figure 1A). The inclusion of the previously described JNK-inhibitory peptide TIJIP (2 μ M; [11]) served as a positive control showing that PYC71N could achieve comparable levels of inhibition under these assay conditions (Figure 1A).

The structural properties of the active PYC71 and PYC71N peptides were therefore explored in greater detail. The secondary structure of PYC71 and PYC71N in the presence and absence of 30% TFE was determined using CD spectroscopy (Figure 1B). CD spectral analysis of PYC71 showed that the peptide comprises approx. 25% α -helix and 13% β -strand with a significant proportion (~46%) of unordered structure (Supplementary Table S1). The inclusion of TFE, which stabilizes hydrogen bonding [25], promoted an increase in β -strand to ~33% with a concomitant decrease in unordered structure to ~25% (Supplementary Table S1). By contrast, the secondary structure of PYC71N was largely unordered (~62%) in aqueous solution with no α -helical structure and approximately 25% β -strand (Supplementary Table S1). The inclusion of TFE stimulated the formation of β structure in PYC71, as well as a small proportion of α -helical structure (~8%) and a significant decrease in the proportion of unordered structure (Supplementary Table S1). Next, we evaluated the quaternary structure of the peptides in aqueous solution using sedimentation equilibrium studies in the analytical ultracentrifuge (Figure 1C). The resulting sedimentation equilibrium profiles of PYC71 and PYC71N were fitted to a single species model, which provided excellent fits (Figure 1C, solid lines) yielding equivalent molecular masses of 2.51 kDa and 1.54 kDa respectively (Supplementary Table S2 at <http://www.BiochemJ.org/bj/434/bj4340399add.htm>). The data thus indicates that both peptides exist as monomers in aqueous solution.

PYC71 and PYC71N show concentration-dependent inhibition of JNK1 activity towards a range of substrate proteins

To define the mechanism of action of PYC71 and PYC71N as JNK-inhibitory peptides, we next evaluated the efficacy of these peptides to inhibit JNK1-mediated phosphorylation of three well

(A) The N-terminal 13 amino acids of PYC71 (PYC71N), but not the middle (PYC71M) or C-terminal (PYC71C) regions, inhibited JNK1 activity towards GST-c-Jun(1-135). Active JNK1 α 1 and GST-c-Jun(1-135) were pre-incubated (5 min, 30°C) with peptide (100 μ M PYC71N, PYC71M, PYC71C, or 2 μ M TIJIP as a positive control). JNK activity was estimated by quantitation of the incorporation of ³²P into GST-c-Jun(1-135) (upper panel) in three independent experiments. Autoradiography indicated the level of phosphorylation of the c-Jun substrate (lower panel). Results were expressed as the percentage of the uninhibited JNK1 activity, where error bars represent the S.E. of the means and asterisks indicate values statistically significantly different ($*P \leq 0.1$, $n = 3$) from the non-inhibited control reaction. (B) CD spectroscopy reveals secondary structural elements of PYC71 and PYC71N. CD spectra [$\Delta\epsilon$ (M⁻¹ cm⁻¹) compared with wavelength (nm)] of JNK inhibitory peptides [0.15 mg/ml PYC71 (○), PYC71 in the presence of 30% TFE (●), PYC71N (△), and PYC71N in the presence 30% TFE (▲)] were recorded from 190 to 240 nm. Raw data were fitted by nonlinear least squares regression (solid lines) using the CDPPro software package [21] and employing the CONTINLL algorithm with the SP22X, SP29, SP37A and SMP56 reference sets respectively. (C) Sedimentation equilibrium analysis of PYC71 (○) and PYC71N (△) at 0.15 mg/ml is consistent with the expected molecular mass of monomeric peptides in solution (Supplementary Table S2 at <http://www.BiochemJ.org/bj/434/bj4340399add.htm>). Data points obtained at a rotor velocity of 50000 rev/min (symbols) were overlaid with the non-linear least squares best fits (solid lines) to a single species (lower panel). Residuals, plotted as a function of radial position (cm) from the axis of rotation for PYC71 (○) and PYC71N (△) (upper panels) demonstrate excellent agreement between the data and the line of best fit.

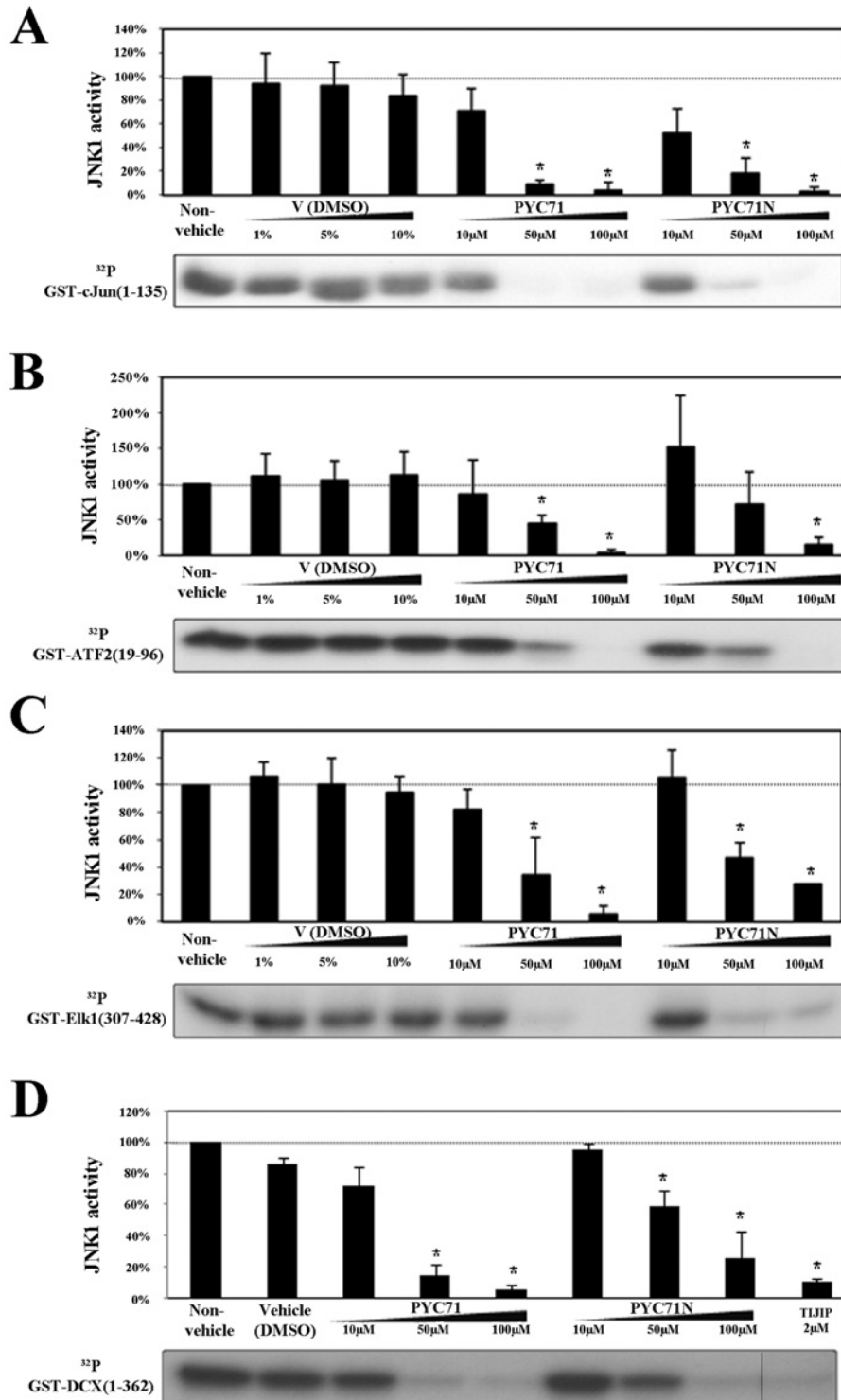


Figure 2 PYC71 and PYC71N show concentration-dependent JNK1 inhibition as determined against a range of substrate proteins

Active JNK1 α 1 and its substrates GST-c-Jun(1-135) (**A**), GST-ATF2(19-96) (**B**), GST-Elk1(307-428) (**C**) or GST-DCX(1-362) (**D**) were pre-incubated (5 min, 30°C) with 10, 50 and 100 μ M peptides (PYC71 or PYC71N) before assaying the kinase activity of JNK1. Incubations in the presence of DMSO at final concentrations of 1, 5 and 10% (equivalent to the levels included for the assays in the presence of 10, 50 and 100 μ M peptide) were included as vehicle controls. For each set of results, autoradiography indicated the level of phosphorylation of each substrate (lower panels), and the incorporation of 32 P into each JNK substrate was quantitated by liquid scintillation counting (upper panels). Results were expressed as the percentage of the uninhibited JNK1 activity in three independent experiments, where error bars represent the standard error of the means and asterisks indicate values statistically significantly different ($*P \leq 0.05$, $n = 3$) from the non-inhibited control reaction.

characterized transcription factor substrates, c-Jun (Figure 2A), ATF2 (Figure 2B) and Elk1 (Figure 2C). In agreement with our previous results testing TIJIP as a JNK-inhibitory peptide, both PYC71 and PYC71N inhibited JNK activity towards all three substrates. Although statistically significant inhibition was observed for a majority of reactions that included 50 μM PYC71 or PYC71N, the most effective inhibition was observed when these peptides were included at a final concentration of 100 μM (Figures 2A–2C).

To extend these studies, we considered whether PYC71 and PYC71N could inhibit JNK activity towards other substrates. A survey of the available literature describing JNK substrates [29] suggested that the microtubule regulatory protein DCX may represent a distinct class of JNK substrate owing to its interaction with JNK via its DCX domains [30]. When we tested JNK1-mediated phosphorylation of DCX, our results clearly showed significant inhibition by PYC71 and PYC71N as well as the TIJIP peptide (Figure 2D). Thus the peptides inhibited JNK activity towards the range of substrates examined.

Inhibition of JNK isoforms JNK1, JNK2 and JNK *in vitro* and c-Jun phosphorylation in cells

To define the effects of PYC71N against different JNK isoforms, we conducted *in vitro* kinase activity assays of JNK1 α 1 (Figure 3A) JNK2 α 2 (Figure 3B) and JNK3 α 1 (Figure 3C) towards the substrate c-Jun. These analyses demonstrated that PYC71N effectively inhibited each of these JNK isoforms in a concentration-dependent manner (Figure 3) and thus that the actions of PYC71N showed no JNK isoform selectivity.

We next tested the PYC71 peptide when conjugated to the TAT cell-permeable delivery peptide, in both its L-amino acid and retroinverso D-amino acid forms, for efficacy in a cultured PC12 cell system (Figure 4). Under these conditions, hyperosmotic stress stimulated an increase in c-Jun Ser⁷³ phosphorylation (Figure 4A, upper panel) and a change in mobility of the total c-Jun protein corresponding with its phosphorylation (Figure 4A, middle panel). Immunoblotting for tubulin indicated comparable levels of protein in all samples (Figure 4A, lower panel). The ATP-competitive inhibitor JNK inhibitor VIII, as well as the protein substrate competitive inhibitory peptide TAT-TIJIP, were included as positive control inhibitors. Both were shown to decrease the hyperosmotic stress-stimulated increase in c-Jun Ser⁷³ phosphorylation under these conditions (Figure 4A, upper panel), albeit that the JNK inhibitor VIII appeared to be more effective in preventing the change in mobility of the total c-Jun protein that follows hyperosmotic stress (Figure 4A, middle panel).

When we examined the effects of TAT-conjugated PYC71 peptides, we noted that 1 μM of either the L-amino acid or retroinverso D-amino amino acid form were not effective in reducing c-Jun Ser⁷³ phosphorylation (Figure 4A, upper panel). However, further increasing the concentration to 10 μM did inhibit c-Jun Ser⁷³ phosphorylation by the L-amino acid form of TAT-conjugated PYC71 (Figure 4A, upper panel). In contrast, a retroinverso D-amino acid form of the TAT-PYC71 peptide (1 or 10 μM) did not inhibit c-Jun phosphorylation under these conditions (Figure 4A, upper panel). When the levels of total c-Jun were also examined, the TAT-conjugated PYC71 peptides did not inhibit the change in mobility during hyperosmotic stress, but rather 10 μM of the peptides further enhanced the presence of the higher mobility forms of c-Jun. These observations suggest that these peptides may promote the phosphorylation of c-Jun at additional sites under the conditions tested. Higher concentrations

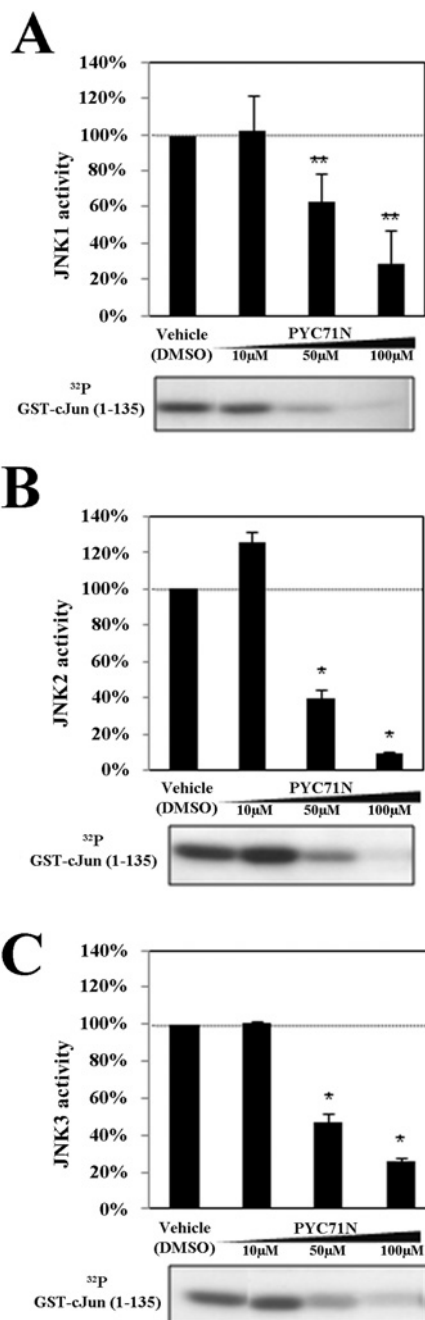


Figure 3 PYC71N inhibits the activity of JNK1, JNK2 and JNK3 isoforms towards c-Jun

Active JNK1 α 1 (A), JNK2 α 2 (B) or JNK3 α 1 (C) and GST-c-Jun(1–135) were pre-incubated (5 min, 30 °C) with 10, 50 and 100 μM PYC71N before assaying the kinase activity of JNK. DMSO (10%) was included as a vehicle control. The incorporation of ³²P into c-Jun was quantitated and results were expressed as a percentage of the uninhibited kinase activity in three independent experiments. Error bars represent the S.E.M. and asterisks indicate values statistically significantly different (* $P \leq 0.1$, ** $P \leq 0.05$, $n = 3$) from the non-inhibited control reactions.

of the peptides could not be tested due to their toxicity in this system (Ng D. and Bogoyevitch M., unpublished work).

Lastly, we examined how exposure to the inhibitors affected JNK phosphorylation following exposure to hyperosmotic stress. The ATP-competitive inhibitor JNK inhibitor VIII, as well as the protein substrate competitive inhibitory peptide TAT-TIJIP did not affect JNK phosphorylation. Despite only the L-amino acid

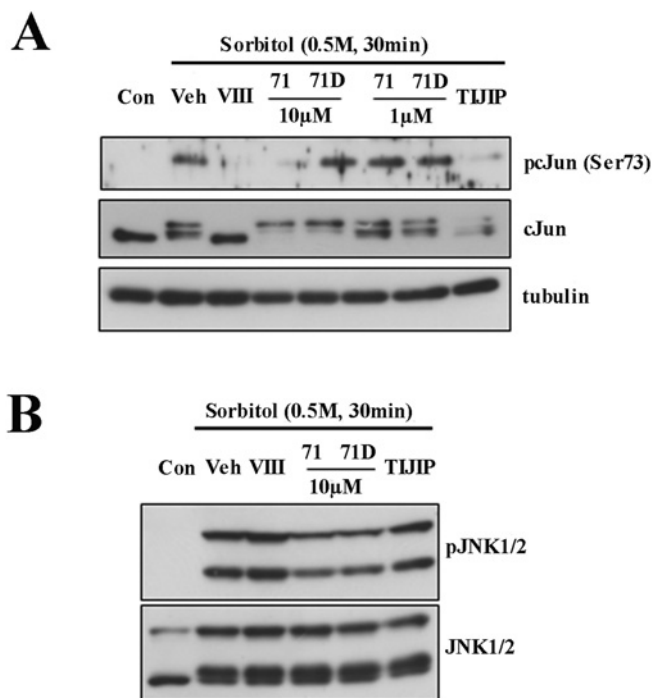


Figure 4 A cell-permeable version of PYC71 can inhibit c-Jun phosphorylation following hyperosmotic stress

PC12 cells were pre-treated with DMSO as vehicle (Veh), JNK inhibitor VIII (VIII), TAT-conjugated TIJIP (TIJIP), TAT-conjugated PYC71 (71) or the D-amino acid form of TAT-conjugated PYC71 (71D) before being treated with sorbitol (0.5 M, 30 min). Protein lysates were prepared and blotted with antibodies against phosphoSer⁷³ c-Jun, total c-Jun and tubulin (**A**), or phosphoJNK1/2 and total JNK1/2 (**B**). Experiments were repeated on two independent occasions with comparable results.

TAT-conjugated PYC71 peptide showing decreased c-Jun Ser⁷³ phosphorylation, both the L-amino acid and the retroinverso D-amino acid forms of the TAT-PYC71 led to small reductions in the levels of JNK phosphorylation detected (Figure 4B). These results therefore further support the actions of the JNK inhibitors to prevent c-Jun Ser⁷³ phosphorylation primarily at the level of JNK activity, rather the phosphorylation/activation of JNK by upstream kinases such as MKK4 and MKK7.

JNK1 inhibition by PYC71N is non-competitive with respect to ATP, but consistent with effects mediated via a protein substrate–inhibitor complex

To explore the mechanism of PYC71N-mediated inhibition of JNK1, we then performed kinetic assays. JNK1 α 1 activity was assayed with either GST–c-Jun(1–135) or various ATP concentrations, at a fixed concentration of the other component in the presence or absence of a range of concentrations of PYC71N (10–40 μ M). Data obtained from the experiments performed at fixed ATP concentration, where GST–c-Jun(1–135) concentrations were varied in the presence of increasing concentrations of PYC71N, were indicative of mixed competitive inhibition (Figure 5A). When similar experiments were performed with constant GST–c-Jun(1–135) concentration, various ATP concentrations and at several concentrations of PYC71N, the inhibition was non-competitive with respect to ATP (Figure 5B).

We then explored the unusual feature of these kinetic results, namely the positive x -intercept shown in the kinetic analysis in Figure 5(A). To better define the possible mechanisms used

by PYC71N, the kinetics data was further analysed by plotting the reaction velocity (v , pmol/min) against the concentration of PYC71N present in the reactions over the range of GST–c-Jun concentrations (Figure 5C). A similar analysis with TIJIP performed in parallel confirmed the protein substrate competitive nature of the observed inhibition, as indicated by a linear relationship between v and amount of inhibitor (Figure 5D). In contrast, the non-linear pattern observed with PYC71N (Figure 5C) was consistent with the inhibitory species in these assays being a substrate–inhibitor complex [31,32].

Alanine-scanning replacement within PYC71N reveals the requirement for an FFX motif

Our previous analyses of the JNK-inhibitory TIJIP peptide identified a critical requirement for four amino acids within the 11 amino acid peptide, each being essential for JNK inhibition [11]. We hypothesized that there could be a similar requirement for a small number of specific amino acids within the PYC71N sequence that would be essential for its JNK-inhibitory actions. By sequentially replacing each of the amino acids within PYC71N with alanine (for the specific sequences of each tested peptide see Supplementary Table S3 at <http://www.BiochemJ.org/bj/434/bj4340399add.htm>), we revealed that Phe⁹ and Phe¹¹ were essential because their individual change to alanine abolished the JNK inhibition (Figure 6A). Furthermore, although the best characterized JBD (JNK-binding domain) motifs have been described to follow the general consensus sequence of (A/K)X_{1–4} ϕ X ϕ (where ϕ represents hydrophobic residues and commonly these are isoleucine or leucine) [17,29,33], we demonstrated no requirement for the N-terminal basic residues (Arg⁴ or Lys⁷) in these analyses (Figure 6A), suggesting that PYC71N forms a new class of JNK-inhibitory peptide.

Further truncation analysis and amino acid replacements highlight features of PYC71N critical for its inhibition of JNK1

To complement the alanine-scanning replacement experiments, we also assayed the inhibition of JNK1 by a series of peptides corresponding to further truncations of PYC71N (Figure 6B). The specific sequences for each tested peptide are summarized in Supplementary Table S3. We found that removal of one or two residues from either the N-terminus or the C-terminus of the peptide did not significantly change JNK inhibition from that observed with PYC71N (Figure 6B). Removal of three to six C-terminal residues resulted in the loss of inhibitory actions, consistent with the alanine-scanning results which highlighted the critical requirement for Phe¹¹ [11]. Similarly, when considering the N-terminal truncation series, the removal of up to four amino acids did not significantly decrease the inhibition by the peptides. However, the loss of five or six of the N-terminal residues resulted in a loss of inhibition even though the remaining peptide sequences retained the critical FFX motif (Phe⁹ and Phe¹¹ residues; Figure 6B). Similarly, when one or two amino acids were simultaneously removed from both the N- and C-terminus, these shorter peptides showed significantly less JNK inhibition when compared with the full length PYC71N (Figure 6B). These results highlight the requirement for a critical peptide length to retain JNK-inhibitory characteristics.

To explore the requirements for specific amino acids within PYC71N in greater detail, we then evaluated changes at five positions: Arg⁴, Leu⁵, Lys⁷, Phe⁹ and Tyr¹⁰. We used three different substitutions (Figure 6C): glycine (to allow maximum conformational flexibility), proline (to minimize conformational

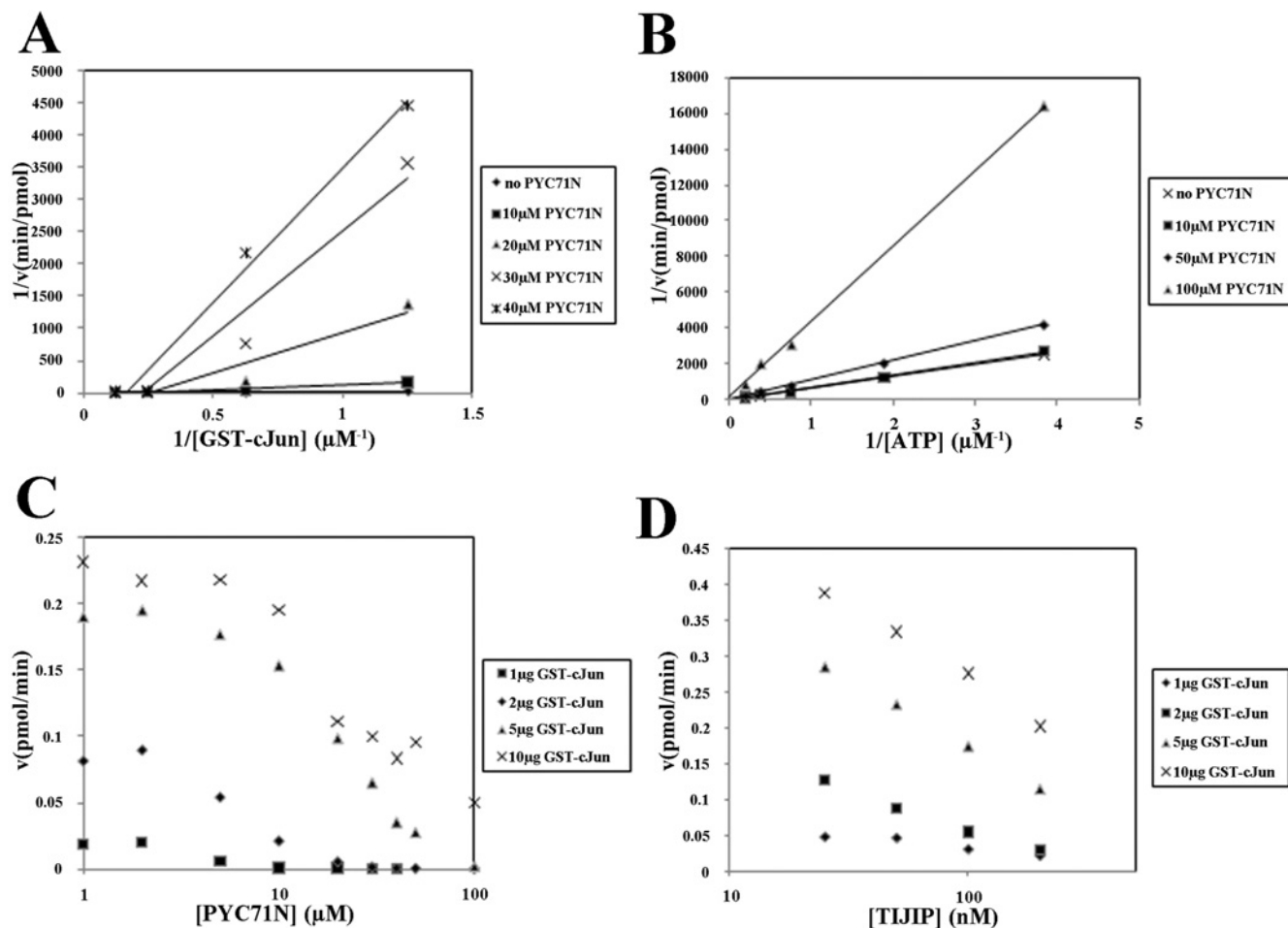


Figure 5 Kinetic characterization studies reveal a novel mechanism of PYC71N-mediated JNK1 inhibition

(A–C) The inhibition of JNK1 α 1 by PYC71N was assessed over a range of substrate concentrations. (A) Inhibition of the activity of JNK1 α 1 towards a range of concentrations of GST–c-Jun(1–135) (0.8–8.1 μ M) by four PYC71N concentrations was determined at a fixed ATP concentration (5.3 μ M). (B) Inhibition of the activity of JNK1 α 1 by three concentrations of PYC71N towards a fixed concentration of GST–c-Jun(1–135) (8.1 μ M) was determined at a range of ATP concentrations (0.26–5.3 μ M). Data was analysed by double-reciprocal plot $\{1/v$ [min/pmol] compared with $1/[GST-c-Jun(1-135)]$ [μ M $^{-1}$] or $1/[ATP]$ [μ M $^{-1}$]} and the lines shown were derived from linear regression analysis. This analysis was consistent with an inactive substrate–inhibitor complex and mixed competitive inhibition. (C and D) The data for JNK1 inhibition by PYC71N were replotted as v against PYC71N (μ M) at 1, 2, 5 and 10 μ g of GST–c-Jun(1–135), and comparable data were plotted for the TIJIP-mediated inhibition of JNK1 as determined in parallel experiments. (C) The non-linear relationship shown for the PYC71N data was consistent with an inactive substrate–inhibitor complex. (D) The linear relationship for the TIJIP data was consistent with inhibition via protein substrate competition.

flexibility) or phenylalanine (to add a bulky hydrophobic residue). The specific sequences for each tested peptide are summarized in Supplementary Table S3. For Arg⁴, the tested changes did not decrease the inhibition significantly when compared with the assays using authentic PYC71N that were performed in parallel (Figure 6C). Similarly, when we tested these changes in the residues between Arg⁴ and the essential Phe⁹, we found these changes were again well tolerated (Figure 6C). The inclusion of glycine or proline residues in place of Phe⁹ decreased the observed inhibition and again reinforced the conclusion of the essential nature of phenylalanine in this position (Figure 6C).

Lastly, in probing the nature of the FFX motif (Phe⁹Tyr¹⁰Phe¹¹), we found that the inclusion of a phenylalanine residue in place of Tyr¹⁰ was well tolerated, but in contrast the inclusion of proline at this position resulted in lower inhibitory actions. Taken together, these results emphasize the requirement for the hydrophobic interactions in mediating JNK inhibition, but further that the inclusion of a residue such as proline within the FFX motif can disrupt JNK-inhibitory actions.

BIAcore-based analyses demonstrate that PYC71N directly binds inactive JNK and c-Jun, and confirm the requirement of the FFX motif for PYC71N inhibitory activity

To further explore the interactions between PYC71N and JNK1, we directly assessed interactions in real time using SPR/BIAcore technology. This is crucial to define whether the action of PYC71N was via its binding JNK or its substrates. Thus we developed a baculovirus/*Sf9* cell expression system to achieve good yields of unphosphorylated, inactive JNK1 protein, which was later confirmed by immunoblotting and CD analysis. Through BIAcore analyses, we demonstrated binding between immobilized PYC71N towards either c-Jun (Figure 7Ai) or JNK1 (Figure 7Aii). Similar interactions between PYC71N and the substrate ATF2 and Elk1 were also demonstrated qualitatively (Ngoei K., Catimel B. and Bogoyevitch M., unpublished work).

To validate the requirement of Phe⁹ and Phe¹¹ for JNK inhibition, we then immobilized PYC71N alanine mutant variants

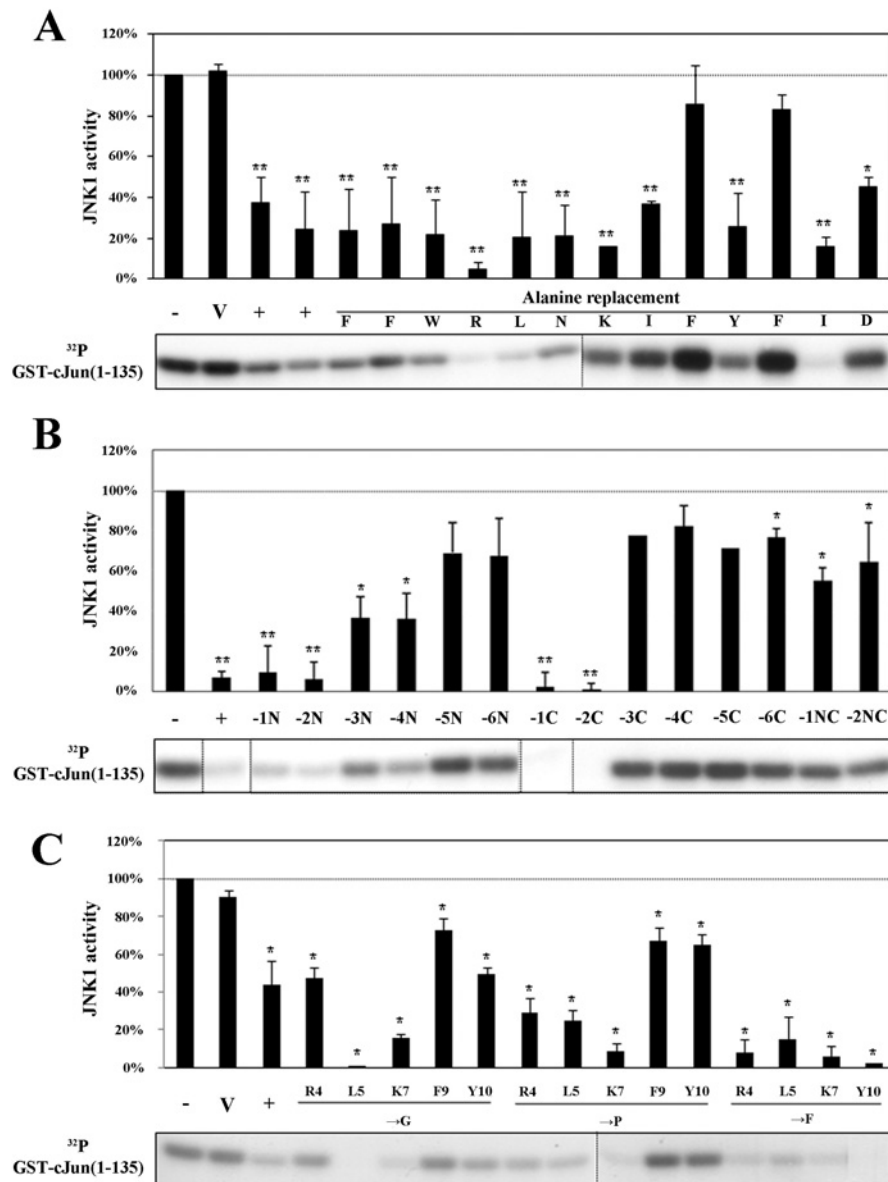


Figure 6 Identification of amino acids and peptide length critical for PYC71N to inhibit JNK1 activity towards c-Jun

Active JNK1 α 1 and GST-c-Jun(1-135) were pre-incubated (5 min, 30 °C) with either alanine-substituted PYC71N peptides (**A**), N-terminal, C-terminal and combined N- and C-terminal truncated versions of the PYC71N peptide (**B**) or glycine-, proline- or phenylalanine-substituted PYC71N peptides (**C**) before assaying JNK1 activity. DMSO at a final concentration of 2.5% was included in the vehicle (V) control. PYC71N was included as a positive (+) control. All bands shown were taken from a single experiment and images were spliced as indicated to simplify viewing. The incorporation of ^{32}P into GST-c-Jun(1-135) was quantitated and results were expressed as a percentage of the uninhibited JNK1 activity in three independent experiments (upper panels). Error bars represent the S.E.M. and asterisks indicate values statistically significantly different ($*P \leq 0.05$, $n = 3$) from the non-inhibited control reaction.

(biotin-PYC71N Phe⁹Ala and biotin-PYC71N Phe¹¹Ala). Interestingly, no binding was detected when c-Jun(1-135) was injected over immobilized PYC71N Phe⁹Ala and PYC71N Phe¹¹Ala (Figures 7Bi and 7Ci respectively), again consistent with the results observed in the previous section which supported the substrate-inhibitor complex model. We then tested if the peptide mutations would reduce its binding to the inactive form of JNK1. From the sensorgrams, inactive JNK1 was observed to bind to PYC71N, PYC71N Phe⁹Ala and Phe¹¹Ala mutants (Figures 7Aii, 7Bii and 7Cii respectively). Kinetic analysis using global fitting with mass transfer model showed that all three proteins displayed similar apparent association and dissociation rates (k_a values from 9.16 to $13.2 \times 10^3 \text{ M}^{-1} \cdot \text{s}^{-1}$, k_d values

ranged from 5.11 to $5.89 \times 10^{-4} \text{ s}^{-1}$) resulting in K_D values ranging from 44.7 to 56.8 nM. However, absolute comparison required the amount of peptide immobilized to be taken into account and calculated as surface molar binding activity, as described in the Materials and methods section [28]. Surface molar binding activity showing relative binding levels of JNK1 with immobilized PYC71N had revealed significant reduction between PYC71N mutant forms (0.017 and 0.023 for Phe⁹Ala and Phe¹¹Ala respectively) as compared with PYC71N (0.032) (Table 2). Taken together, these observations again highlight the importance of Phe⁹ and Phe¹¹, and that mutation of either residue abolishes peptide binding to c-Jun. These results are consistent with the substrate-inhibitor complex model of JNK inhibition.

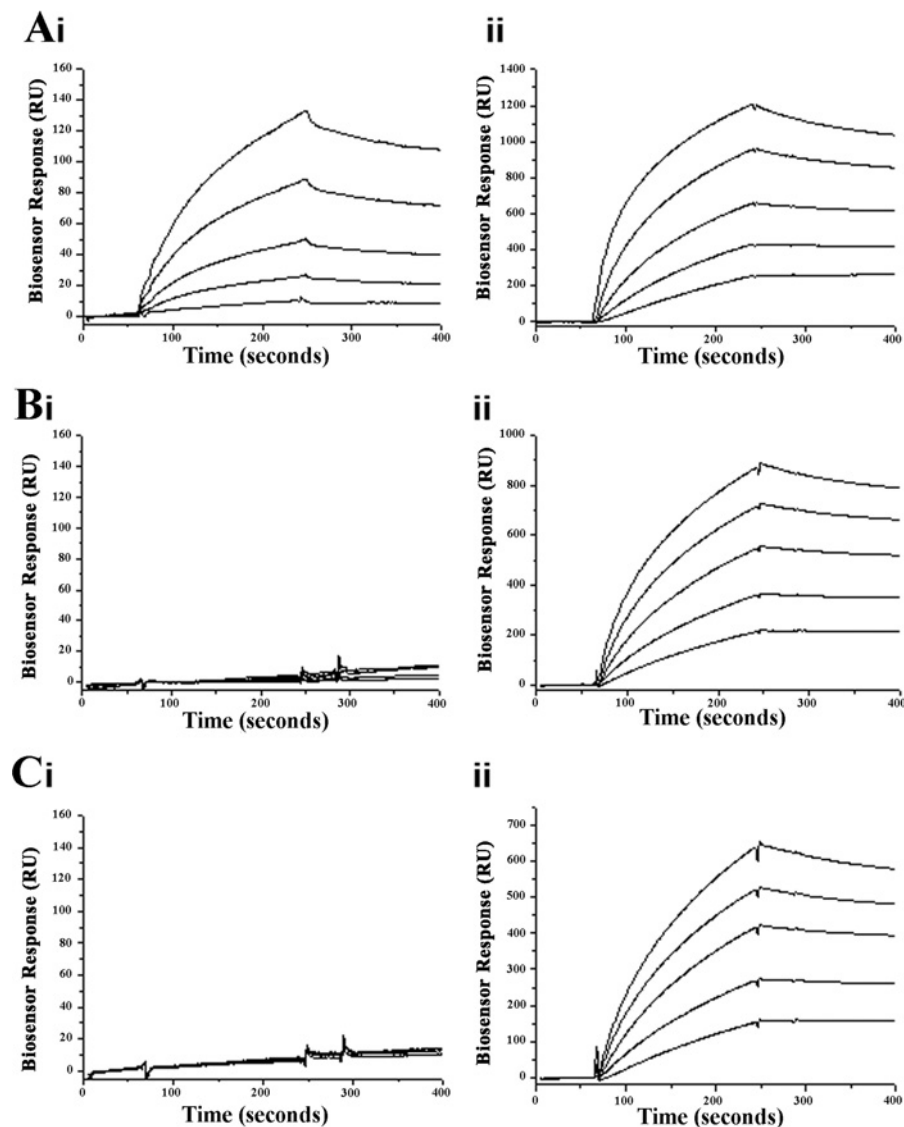


Figure 7 PYC71N interaction with c-Jun is consistent with a substrate–inhibitor complex mechanism

The interaction between JNK1 α 1, c-Jun(1–135) and immobilized PYC71N was analysed by BIAcore. Injection of c-Jun(1–135) (i) and JNK1 α 1 (2.3 μ M, 1.15 μ M, 0.58 μ M, 0.29 μ M and 0.14 μ M) (ii) over immobilized PYC71N (1.6 ng/mm²) (A), PYC71N Phe⁹Ala (2.0 ng/mm²) (B) and PYC71N Phe¹¹Ala (1.2 ng/mm²) (C).

Table 2 Relative binding levels of JNK1 with immobilized PYC71N variants

Peptide	Peptide immobilized (RU)	Detector signal (RU)	Relative response (RU/RU)	Surface molar binding activity
PYC71N	1583	1103	0.70	0.032
PYC71N Phe ⁹ Ala	2021	756	0.37	0.017
PYC71N Phe ¹¹ Ala	1173	619	0.53	0.023

BIAcore analyses reveal that unlike TIJIP, PYC71N does not interact with active JNK1

To evaluate whether the activation status of JNK1 may influence the extent of peptide binding, we then conducted BIAcore analyses of PYC71N in parallel with the peptide TIJIP. In the baculovirus/*Sf9* cell expression system, we co-expressed GST–JNK1 α 1 with the upstream kinases MKK4 and MKK7 to generate phosphorylated active JNK1. The expression of active JNK1 α 1,

as determined by immunoblotting for phosphorylated JNK, CD spectra of the JNK protein and activity towards c-Jun (Ngoei K. and Bogoyevitch M., unpublished work), had confirmed the integrity and activity of the purified JNK1 α 1 protein. Through BIAcore analyses, we demonstrated binding between immobilized PYC71N and TIJIP towards JNK1 (Figures 8A–8D). We began by examining the interaction of the characterized TIJIP peptide with either inactive (Figure 8A) or active (Figure 8C) JNK1 α 1, showing that the extent of maximal binding was

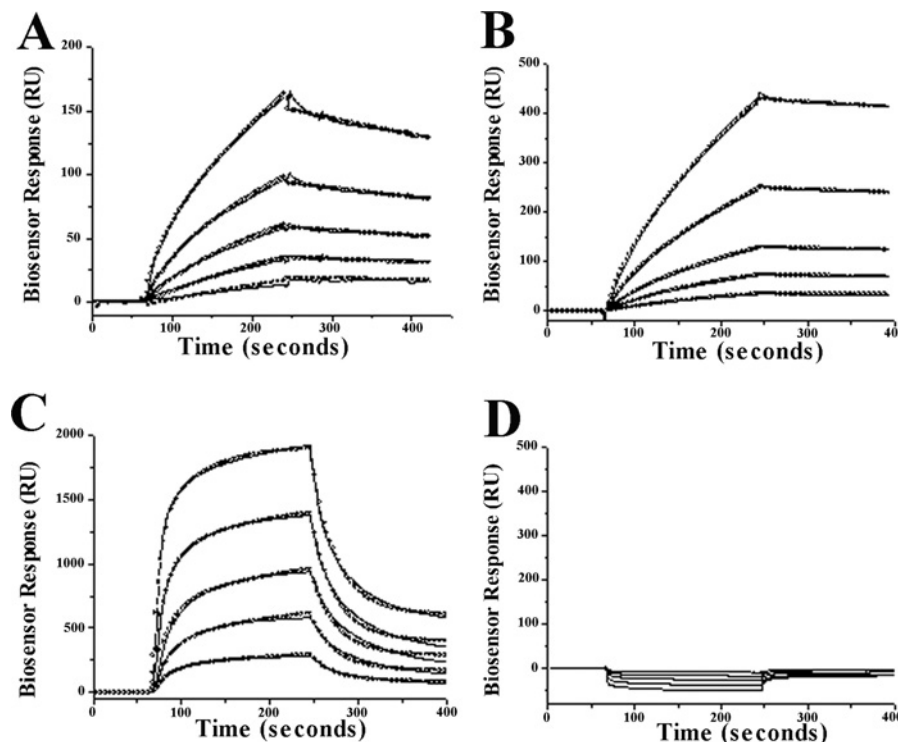


Figure 8 Interaction analysis reveals that JNK1 activation changes its peptide interactions

The interaction between JNK1 α 1 and immobilized peptides (PYC71N or TIJIP) was analyzed by BIAcore. Injection of JNK1 α 1 purified in its inactive form (4.2 μ M, 2.1 μ M, 1.05 μ M, 525 nM and 262.5 nM) over immobilized biotinylated TIJIP (0.6 ng/mm² RU) (A) or immobilized biotinylated PYC71N (0.8 ng/mm²) (B). Injection of JNK1 α 1 purified in its active form (1.7 μ M, 850 nM, 425 nM, 212.5 nM and 106.2 nM) over immobilized biotinylated TIJIP (0.6 ng/mm²) (C) or immobilized biotinylated PYC71N (0.8 ng/mm²) (D). The experimental (solid line) and fitted data (circles) using global analysis using a heterogeneous ligand model are indicated.

increased for the active form of JNK1 α 1 [Rmax (maximum analyte binding capacity) of 2616 RU (response units) using global fitting] compared with inactive JNK1 α 1 (Rmax of 215 RU using global fitting). Furthermore, inactive JNK1 α 1 was shown to interact with immobilized PYC71N (Figure 8B). Strikingly, no interaction of the active form of JNK1 α 1 with PYC71N was detected (Figure 8D). As PYC71N interacted with c-Jun(1–135), these data again supported the substrate–inhibitor complex model for the mechanism of PYC71N-mediated inhibition of JNK activity.

We analysed our data quantitatively with kinetic constants derived from the sensorgrams with BIAEVALUATION 4.1 software (Table 3). Binding curves were first fit with a 1:1 Langmuir model using the regions of the dissociation and association phases where Langmuir interactions appeared to be operative (separate k_a and k_d fitting). Simultaneous evaluation of k_a and k_d were also performed using global fitting protocols (1:1 binding with mass transfer and heterogeneous ligand model). Calculated apparent association (k_{a1}) and dissociation (k_{d1}) rates were consistent in all three models resulting in similar K_{D1} values. Analysis of the interaction between inactive JNK1 and TIJIP gave apparent association rates ranging from 3.0 to $1.1 \times 10^3 \text{ M}^{-1} \cdot \text{s}^{-1}$ and apparent dissociation rates values from 22.2 to $13.2 \times 10^{-4} \text{ s}^{-1}$ (Table 3). These values resulted in a high nM/low μ M binding affinity (the calculated K_{D1} ranging from 740 nM to 1.2 μ M).

Higher apparent on- and off-rate values (k_{a1} ranging from 156 to $101 \times 10^3 \text{ M}^{-1} \cdot \text{s}^{-1}$ and k_{d1} ranging from 353 to $213 \times 10^{-4} \text{ s}^{-1}$) were generated in the analysis of the interaction between active JNK1 α 1 and the immobilized TIJIP peptide (Table 3). These values resulted in low nM affinity constant (K_{D1} ranging from 136 nM to 350 nM). The 1:1 Langmuir analyses for PYC71N

binding to inactive JNK1 α 1 indicated apparent k_{a1} values of $2.7 \times 10^3 \text{ M}^{-1} \cdot \text{s}^{-1}$ comparable with those observed for binding to TIJIP, but lower k_{d1} values ($k_{d1} = 6.2 \times 10^{-4} \text{ s}^{-1}$) and thus decreasing the calculated K_{D1} value for this interaction model (229 nM). This reduction in K_{D1} was generally observed on all three binding models (ranging from 188 nM to 380 nM) (Table 3). The lack of interaction of active JNK1 α 1 with PYC71N (Figure 8D) precluded any further quantitative analysis. Taken together, these data further reiterate the differences in the actions of these two JNK-inhibitory peptides.

Using both 1:1 Langmuir and global fitting models, we investigated the kinetic constants on PYC71N interaction with c-Jun(1–135) (Table 3). Similarly, the calculated association (k_{a1}) and dissociation (k_{d1}) values were in agreement (ranging from 0.9 to $0.6 \times 10^3 \text{ M}^{-1} \cdot \text{s}^{-1}$ for k_{a1} and 9.2 to $7.5 \times 10^{-4} \text{ s}^{-1}$ for k_{d1} values), and resulted in similar K_{D1} values ranging from 1000 nM (Global Fitting heterogeneous ligand) to 1250 nM (1:1 Langmuir) (Table 3).

BIAcore analysis reveals the mechanism of PYC71N peptide by inhibiting the binding of JNK to c-Jun

To further investigate the mechanism of PYC71N inhibitory actions, we conducted BIAcore competition binding experiments by studying the binding of JNK1 to immobilized GST–c-Jun(1–135) in the presence or absence of PYC71N peptides (Figure 9). Stable levels of PYC71N peptides (0.05 ng/mm² and 0.2 ng/mm²) bound to GST–c-Jun(1–135) (immobilization level of 12 ng/mm²) were achieved after peptide injection and

Table 3 Kinetic parameters for the interactions of JNK-inhibitory peptides with JNK1 α 1 and c-Jun(1–135)

Recombinant JNK1 α 1 was produced in *Sf9* cells following infection with baculovirus encoding GST–JNK1 α 1 either alone (inactive JNK1 α 1) or in combination with baculovirus encoding MKK4 and MKK7 (active JNK1 α 1). GST–JNK was then purified using standard GSH–Sepharose affinity followed by ion-exchange chromatography and the GST was removed by PreScission protease cleavage prior to use in the biosensor experiments. GST–c-Jun(1–135) was expressed in the bacterial protein expression system and the GST tag was removed via thrombin cleavage. Kinetic constants were derived from the resulting sensorgrams with BIAEVALUATION 4.1 software (BIAcore). K_{D1} is the predominant dissociation constant for the interaction indicated from the relative amplitudes obtained by non-linear least squares regression analysis using a double exponential form of the rate equation. K_{D1} percentage of the total signal is indicated in brackets.

Protein/peptide	Analysis model	Kinetic constants						χ^2
		$k_{a1} \times 10^{-3}$ ($M^{-1} \cdot s^{-1}$)	$k_{d1} \times 10^4$ (s^{-1})	$K_{D1} \times 10^9$ (M)	$k_{a2} \times 10^{-3}$ ($M^{-1} \cdot s^{-1}$)	$k_{d2} \times 10^4$ (s^{-1})	$K_{D2} \times 10^9$ (M)	
Inactive JNK1/immobilized TJJP	1/1 Langmuir association Separate k_a/k_d	3.0	22.2	740		0.2		
	Global fitting simultaneous k_a/k_d 1/1 binding with mass transfer	2.1	17.5	833		4.4		
	Global fitting simultaneous k_a/k_d heterogeneous ligand model	1.1	13.2	1200 (91%)	6.3	4.5	70	4.5
Active JNK1/immobilized TJJP	1/1 Langmuir association Separate k_a/k_d	156	213	136		5.1		
	Global fitting simultaneous k_a/k_d 1/1 binding with mass transfer	Poor fit observed						
	Global fitting simultaneous k_a/k_d heterogeneous ligand model	101	353	350 (72%)	3.5	2.4	68	127
Inactive JNK1/immobilized PYC71N	1/1 Langmuir association Separate k_a/k_d	2.7	6.2	229		1.4		
	Global fitting simultaneous k_a/k_d 1/1 binding with mass transfer	1.7	3.2	188		33		
	Global fitting simultaneous k_a/k_d heterogeneous ligand model	1.0	3.8	380 (94%)	23.5	0.24	10	1.6
c-Jun/immobilized PYC71N	1/1 Langmuir association Separate k_a/k_d	0.6	7.5	1250		0.09		
	Global fitting simultaneous k_a/k_d 1/1 binding with mass transfer	0.9	9.2	1022		2.51		
	Global fitting simultaneous k_a/k_d heterogeneous ligand model	0.9	9.0	1000 (50%)	0.8	0.9	1125	1.16

baseline stabilization. JNK1 was then injected at a concentration of 3.3 μ M over GST–c-Jun or GST–c-Jun/PYC71N peptides. Binding of 203 RU was observed when JNK1 was injected in the absence of peptide PYC71N (Figure 9, sensorgram 1). Injection of 0.05 ng/mm² PYC71N reduced the binding of JNK1 to 160 RU (Figure 9, sensorgram 2), while at 0.2 ng/mm² PYC71N the binding response was further reduced to 140 RU (Figure 9, sensorgram 3). Overall, this observation has revealed a mechanism of action of PYC71N peptide also consistent with the substrate–inhibitor complex acting as the inhibitory species.

DISCUSSION

Since their discovery as stress-activated protein kinases in the 1990s, the JNKs have continued to attract attention with their implication in various physiological processes and disease states [7,34]. Significant insights have resulted from an increasing number of *in vivo* studies in *jnk*-knockout mice [35], including the possible roles for JNK in diabetes [36] and neurodegeneration [37], and so there is sustained interest in the development of JNK-specific inhibitors both as biological tools and as possible therapeutic leads [38]. Although the anthrapyrazolone known commonly as SP600125 was the first small molecule ATP-competitive JNK inhibitor to be available commercially [8], the widespread use of this inhibitor has also attracted considerable controversy due to the number of other protein kinases it also targeted [39,40]. Thus there is a continued need to consider

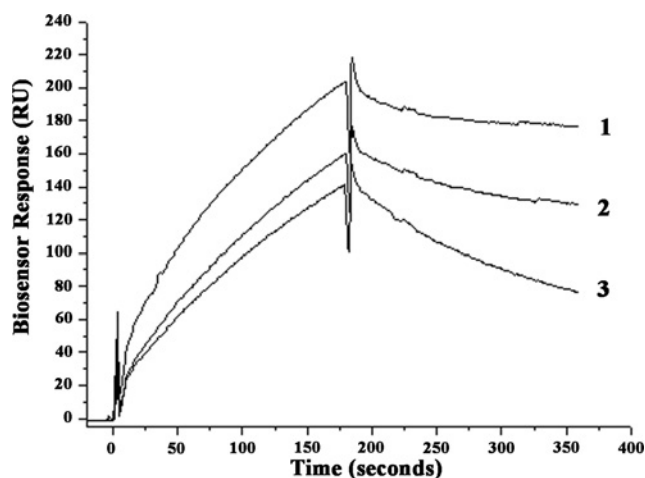


Figure 9 PYC71N peptide inhibited the binding of c-Jun to JNK

The interaction between JNK1 α 1 and GST–c-Jun(1–135) in the presence of PYC71N peptide was examined by BIAcore. Injection of JNK1 α 1 (3.3 μ M) over immobilized GST–c-Jun(1–135) (12 ng/mm²) in the absence of PYC71N (sensorgram 1), in the presence of 0.05 ng/mm² PYC71N (sensorgram 2) and 0.2 ng/mm² PYC71N (sensorgram 3).

the development of alternative JNK inhibitors, both for use in biological studies and also to probe the biochemistry of JNK actions further.

An overarching goal of our laboratory has been to develop and characterize ATP-non-competitive inhibitors of JNK. Previously, we defined a small region of the JIP1 scaffold as a JNK-interacting and inhibitory peptide [11,41,42]. This peptide, referred to here as TIJIP, has provided an excellent alternative to inhibit JNK for studies addressing the roles of JNK both in cells and *in vivo* [13,14,43], as well as probing the biochemistry of JNK-mediated substrate phosphorylation further [44–46] and providing information on the substrate docking site now targeted by a range of small molecule ATP-non-competitive JNK inhibitors [15–18].

We have extended our analysis of TIJIP, including this peptide in parallel studies as a control during our characterization of the novel JNK-inhibitory peptide PYC71N. Our analyses have revealed for the first time that the phosphorylation/activation of JNK1 α 1 markedly enhances its affinity of binding to TIJIP. This observation was facilitated with our development of a baculovirus/*Sf9* cell recombinant protein expression system, in which the co-expression of JNK1 α 1 with the upstream MKKs MKK4 and MKK7, allowed the purification of active JNK1 α 1 in quantities suitable for biophysical interaction analyses. Conversely, the interaction of the novel JNK inhibitory peptide PYC71N was abolished following the activation of JNK1 α 1, pointing to a new mode of action of this JNK inhibitory peptide. The structural alterations underlying these significant changes in binding to these two peptides cannot currently be assessed directly, as the structures of active phosphorylated JNK1 α 1 (or any other isoform of JNK) are not yet available in the public domain. The structures of the JNK1 complex with TIJIP (PDB codes 1UKH and 1UKI) have only been achieved with an inactive (and truncated) form of JNK1 [12]. It will be important for future studies to address these activation-dependent structural changes in JNK1 α 1 and how these increase the binding affinity of JNK for TIJIP. Such studies will also have ramifications for the design and discovery of small molecule inhibitors that target this JNK/TIJIP interaction interface [15–18].

The prime focus of the current study has been the novel peptide PYC71. This peptide was first identified in yeast two-hybrid analysis and analysed in the search for new peptides to exploit for neuroprotective properties [20]. A version of PYC71, made cell-permeable by the inclusion of the TAT delivery peptide, was shown to be without significant effect to prevent neuronal death *in vitro* [20], however this lack of effect may be due to a number of additional factors including differences in the cell permeability of the different peptide species, different subcellular localization and/or additional binding partners, or the intrinsic stability/protease insensitivity of these different peptide sequences during the time course studied in the neuroprotection assays. In the present study, both L-amino acid form and D-amino acid retroinverso form of the PYC71 peptide [20] were tested at 1 and 10 μ M for their actions to inhibit the JNK-mediated phosphorylation of c-Jun that occurs during acute hyperosmotic stress. Whilst 10 μ M of the L-amino acid form could decrease c-Jun Ser⁷³ phosphorylation under these conditions, the 10 μ M D-amino acid retroinverso form was largely without effect on c-Jun Ser⁷³ phosphorylation, suggesting that the potential improvements in intracellular stability afforded by the use of D-amino acids during the synthesis have compromised efficacy of the peptide as a JNK inhibitor. This strategy has been previously examined for the synthesis of TAT–TIJIP when the use of D-amino acid retroinverso peptides were acknowledged to increase inhibitor stability, but with a substantial decrease in inhibitor potency [47]. Unfortunately, further increasing the concentrations of peptides in the present studies in PC12 cells was not possible due to toxicity of these TAT-conjugated PYC71 peptides (Ngoei K., Ng D. and Bogoyevitch M., unpublished work). Furthermore, the actions of

the TAT-conjugated PYC71 peptides to alter the mobility of c-Jun and to produce small decreases in JNK phosphorylation during hyperosmotic stress require further evaluation.

In considering the 22 amino acid sequence of PYC71, we noted the efficacy of the shorter TIJIP (11 amino acids) to inhibit JNK activity. Through testing of fragments of PYC71 (PYC71N, PYC71M and PYC71C, representing 13 amino acids spanning the N-terminal, middle and C-terminal amino acids respectively), we showed that the N-terminal region retained in PYC71N was essential for inhibition. Indeed, JNK1, JNK2 and JNK3 were all effectively inhibited by PYC71N. Kinetic analysis exploring the mechanism of JNK-inhibitory action of PYC71N confirmed the ATP-non-competitive nature of the inhibition. This analysis also pointed to a substrate–inhibitor complex being the effective inhibitory species. This interpretation was further strengthened with the direct observations of PYC71N interaction with c-Jun, but the lack of interaction of this peptide with phosphorylated active JNK under the same conditions *in vitro*. Overall, these findings are consistent with the proposed mechanism of PYC71N binding to c-Jun and inhibiting its interaction with JNK1.

Furthermore, we identified an essential FXF motif as critical for JNK inhibition, as the loss of either phenylalanine residue (Phe⁹ or Phe¹¹) within the context of PYC71N, was sufficient to abolish JNK-inhibitory actions. These observations were again supported by the lack of interactions between PYC71N alanine mutants and c-Jun(1–135). Therefore this has emphasized the essential requirement for hydrophobic residues in mediating JNK inhibition, consistent with our previous findings of an essential LXL motif in TIJIP [11,41]. Strikingly, a requirement for N-terminal basic residues in the JNK-inhibitory actions of PYC71N was discounted in the present studies when the substitution of Arg⁴ or Lys⁷ by either alanine, glycine, proline or phenylalanine residues did not significantly decrease the JNK inhibition by these PYC71N variants. It is tempting to draw analogies between the requirement for the FXF motif in PYC71N and the FXFP motif known to engage the related MAPK ERK2 [33]. Indeed, in testing the efficacy of the PYC71N peptide for inhibition of closely related MAPKs that overlap with JNK in their substrate preferences, we have seen significant albeit less potent inhibition of ERK2 towards Elk and p38 α towards ATF2 in our initial *in vitro* kinase assays (Supplementary Figure S1 at <http://www.BiochemJ.org/bj/434/bj4340399add.htm>). This extends the possibility that the targeting of PYC71N to these substrates will provide a different biological profile through possible disruption of multiple kinase-mediated events. This is a distinct difference from the TIJIP peptide that targets the substrate docking site and thus does not inhibit ERK or p38 activities (Supplementary Figure S1).

Finally, it appears that few currently described inhibitors against any classes of enzymes have demonstrated mechanisms of action via forming an effective inhibitor–substrate complex. We propose that this paucity of additional examples of inhibitors in this class may at least partially reflect the approaches taken to identify novel inhibitors. For example, in the area of protein kinase inhibitor discovery, assay protocols for inhibitors may be biased towards ATP-competitive inhibitors by their inclusion of high protein substrate concentrations and low ATP concentrations [48]. Although the development of new chemical libraries for kinase inhibitor screening will provide new opportunities to discover novel classes of protein kinase inhibitors [49], we now also propose that approaches directed towards substrate targeting have the potential to identify different enzyme inhibitor classes. For JNK, PYC71N therefore represents a novel peptide that will facilitate the exploration of the biochemistry and functions of JNK.

AUTHOR CONTRIBUTION

Marie Bogoyevitch, Kevin Ngoei, Bruno Catimel, Paul Watt and Dominic Ng conceived the study. Marie Bogoyevitch, Kevin Ngoei, Bruno Catimel, Con Dogovski, Matthew Perugini and Heung-Chin Cheng analysed data and wrote the paper. Nicole Church and Bruno Catimel performed interaction experiments, Daisy Lio and Heung-Chin Cheng performed the production of baculovirus-expressed protein, and Con Dogovski and Matthew Perugini performed the biophysical characterization of the peptides. Dominic Ng generated and interpreted the cell-based data.

ACKNOWLEDGEMENTS

We thank Dr O. Reiner (Weizman Institute of Science, Rehovot, Israel) for the GST–DCX expression construct used in the JNK activity assays, and Dr R.K. Barr (University of Western Australia, Crawley, WA, Australia) for initial identification of the action of PYC71 to inhibit JNK1.

FUNDING

K.R.W.N. is supported by a Melbourne International Research Scholarship. D.C.H.N. is supported by a joint-funded National Heart Foundation and National Health and Medical Research Council (NHMRC) Fellowship. M.A.P. acknowledges the Australian Research Council (ARC) for Future Fellowship support. This work has been supported by the NHMRC [grant number 566804] and the ARC [grant number DP0984225].

REFERENCES

- Kyriakis, J. M., Brautigan, D. L., Ingebritsen, T. S. and Avruch, J. (1991) pp54 microtubule-associated protein-2 kinase requires both tyrosine and threonine phosphorylation for activity. *J. Biol. Chem.* **266**, 10043–10046
- Kyriakis, J. M., Banerjee, P., Nikolakaki, E., Dai, T., Rubie, E. A., Ahmad, M. F., Avruch, J. and Woodgett, J. R. (1994) The stress-activated protein kinase subfamily of c-Jun kinases. *Nature* **369**, 156–160
- Barr, R. K. and Bogoyevitch, M. A. (2001) The c-Jun N-terminal protein kinase family of mitogen-activated protein kinases (JNK MAPKs). *Int. J. Biochem. Cell Biol.* **33**, 1047–1063
- Hirosumi, J., Tuncman, G., Chang, L., Gorgun, C. Z., Uysal, K. T., Maeda, K., Karin, M. and Hotamisligil, G. S. (2002) A central role for JNK in obesity and insulin resistance. *Nature* **420**, 333–336
- Yang, D. D., Kuan, C.-Y., Whitmarsh, A. J., Rincon, M., Zheng, T. S., Davis, R. J., Rakic, P. and Flavell, R. A. (1997) Absence of excitotoxicity induced apoptosis in the hippocampus of mice lacking the *Jnk3* gene. *Nature* **389**, 865–870
- Schattenberg, J. M., Singh, R., Wang, Y., Lefkowitz, J. H., Rigoli, R. M., Scherer, P. E. and Czaja, M. J. (2006) Jnk1 but not jnk2 promotes the development of steatohepatitis in mice. *Hepatology* **43**, 163–172
- Bogoyevitch, M. A. and Arthur, P. G. (2008) Inhibitors of c-Jun N-terminal kinases: JuNK no more? *Biochim. Biophys. Acta* **1784**, 76–93
- Bennett, B. L., Sasaki, D. T., Murray, B. W., O'Leary, E. C., Sakata, S. T., Xu, W., Leisten, J. C., Motiwala, A., Pierce, S., Satoh, Y. et al. (2001) SP600125, an anthrapyrazolone inhibitor of Jun N-terminal kinase. *Proc. Natl. Acad. Sci. U.S.A.* **98**, 13681–13686
- Carboni, S., Hiver, A., Szyndralewicz, C., Gaillard, P., Gotteland, J. P. and Vitte, P. A. (2004) AS601245 [1,3-benzothiazol-2-yl-{2-[(2-(3-pyridinyl) ethyl] amino}-4-pyrimidinyl) acetonitrile]: a c-Jun NH₂-terminal protein kinase inhibitor with neuroprotective properties. *J. Pharmacol. Exp. Ther.* **310**, 25–32
- Szczepankiewicz, B. G., Kosogof, C., Nelson, L. T., Liu, G., Liu, B., Zhao, H., Serby, M. D., Xin, Z., Liu, M., Gum, R. J. et al. (2006) Aminopyridine-based c-Jun N-terminal kinase inhibitors with cellular activity and minimal cross-kinase activity. *J. Med. Chem.* **49**, 3563–3580
- Barr, R. K., Kendrick, T. S. and Bogoyevitch, M. A. (2002) Identification of the critical features of a small peptide inhibitor of JNK activity. *J. Biol. Chem.* **277**, 10987–10997
- Heo, Y. S., Kim, S. K., Seo, C. I., Kim, Y. K., Sung, B. J., Lee, H. S., Lee, J. I., Park, S. Y., Kim, J. H., Hwang, K. Y. et al. (2004) Structural basis for the selective inhibition of JNK1 by the scaffolding protein JIP1 and SP600125. *EMBO J.* **23**, 2185–2195
- Borsello, T., Clarke, P. G., Hirt, L., Vercelli, A., Repici, M., Schorderet, D. F., Bogousslavsky, J. and Bonny, C. (2003) A peptide inhibitor of c-Jun N-terminal kinase protects against excitotoxicity and cerebral ischemia. *Nat. Med.* **9**, 1180–1186
- Kaneto, H., Nakatani, Y., Miyatsuka, T., Kawamori, D., Matsuoka, T. A., Matsuhisa, M., Kajimoto, Y., Ichijo, H., Yamasaki, Y. and Hori, M. (2004) Possible novel therapy for diabetes with cell-permeable JNK-inhibitory peptide. *Nat. Med.* **10**, 1128–1132
- De, S. K., Chen, L. H., Stebbins, J. L., Machleidt, T., Riel-Mehan, M., Dahl, R., Chen, V., Yuan, H., Barile, E., Emdadi, A. et al. (2009) Discovery of 2-(5-nitrothiazol-2-ylthio)benzo[d]thiazoles as novel c-Jun N-terminal kinase inhibitors. *Bioorg. Med. Chem.* **17**, 2712–2717
- De, S. K., Stebbins, J. L., Chen, L. H., Riel-Mehan, M., Machleidt, T., Dahl, R., Yuan, H., Emdadi, A., Barile, E., Chen, V. et al. (2009) Design, synthesis, and structure-activity relationship of substrate competitive, selective, and *in vivo* active triazole and thiaziazole inhibitors of the c-Jun N-terminal kinase. *J. Med. Chem.* **52**, 1943–1952
- Stebbins, J. L., De, S. K., Machleidt, T., Becattini, B., Vazquez, J., Kuntzen, C., Chen, L. H., Cellitti, J. F., Riel-Mehan, M., Emdadi, A. et al. (2008) Identification of a new JNK inhibitor targeting the JNK/JIP interaction site. *Proc. Natl. Acad. Sci. U.S.A.* **105**, 16809–16813
- Chen, T., Kablaoui, N., Little, J., Timofeevski, S., Tschantz, W. R., Chen, P., Feng, J., Charlton, M., Stanton, R. and Bauer, P. (2009) Identification of small-molecule inhibitors of the JIP/JNK interaction. *Biochem. J.* **420**, 283–294
- Watt, P. M. (2006) Screening for peptide drugs from the natural repertoire of biodiverse protein folds. *Nat. Biotechnol.* **24**, 177–183
- Meade, A. J., Meloni, B. P., Cross, J., Bakker, A. J., Fear, M. W., Mastaglia, F. L., Watt, P. M. and Knuckey, N. W. (2010) AP-1 inhibitory peptides are neuroprotective following acute glutamate excitotoxicity in primary cortical neuronal cultures. *J. Neurochem.* **112**, 258–270
- Vistica, J., Dam, J., Balbo, A., Yikilmaz, E., Mariuzza, R. A., Rouault, T. A. and Schuck, P. (2004) Sedimentation equilibrium analysis of protein interactions with global implicit mass conservation constraints and systematic noise decomposition. *Anal. Biochem.* **326**, 234–256
- Schuck, P. (2000) Size-distribution analysis of macromolecules by sedimentation velocity ultracentrifugation and lamm equation modeling. *Biophys. J.* **78**, 1606–1619
- Ng, D. C., Zhao, T. T., Yeap, Y. Y., Ngoei, K. R. and Bogoyevitch, M. A. (2010) c-Jun N-terminal kinase phosphorylation of stathmin confers protection against cellular stress. *J. Biol. Chem.* **285**, 29001–29013
- Kendrick, T. S., Lipscombe, R. J., Rausch, O., Nicholson, S. E., Layton, J. E., Goldie-Cregan, L. C. and Bogoyevitch, M. A. (2004) Contribution of the membrane-distal tyrosine in intracellular signaling by the granulocyte colony-stimulating factor receptor. *J. Biol. Chem.* **279**, 326–340
- Yeap, Y. Y., Ng, I. H., Badrian, B., Nguyen, T. V., Yip, Y. Y., Dhillon, A. S., Mutsaers, S. E., Silke, J., Bogoyevitch, M. A. and Ng, D. C. (2010) c-Jun N-terminal kinase/c-Jun inhibits fibroblast proliferation by negatively regulating the levels of stathmin/oncoprotein 18. *Biochem. J.* **430**, 345–354
- Nice, E. C. and Catimel, B. (1999) Instrumental biosensors: new perspectives for the analysis of biomolecular interactions. *BioEssays* **21**, 339–352
- Khalifa, M. B., Choulier, L., Lortat-Jacob, H., Altschuh, D. and Vernet, T. (2001) BIACORE data processing: an evaluation of the global fitting procedure. *Anal. Biochem.* **293**, 194–203
- Catimel, B., Nerrie, M., Lee, F. T., Scott, A. M., Ritter, G., Welt, S., Old, L. J., Burgess, A. W. and Nice, E. C. (1997) Kinetic analysis of the interaction between the monoclonal antibody A33 and its colonic epithelial antigen by the use of an optical biosensor. A comparison of immobilisation strategies. *J. Chromatogr. A* **776**, 15–30
- Bogoyevitch, M. A. and Kobe, B. (2006) Uses for JNK: the many and varied substrates of c-Jun N-terminal kinases. *Micro. Mol. Biol. Rev.* **70**, 1061–1095
- Gdalyahu, A., Ghosh, I., Levy, T., Sapir, T., Sapoznik, S., Fishler, Y., Azoulai, D. and Reiner, O. (2004) DCX, a new mediator of the JNK pathway. *EMBO J.* **23**, 823–832
- Segel, I. H. (1975) *Enzyme Kinetics. Behavior and Analysis of Rapid Equilibrium and Steady-State Enzyme Kinetics.* John Wiley and Sons, New York
- Copeland, R. A. and Horiuchi, K. Y. (1998) Kinetic effects due to nonspecific substrate-inhibitor interactions in enzymatic reactions. *Biochem. Pharmacol.* **55**, 1785–1790
- Akella, R., Moon, T. M. and Goldsmith, E. J. (2008) Unique MAP kinase binding sites. *Biochim. Biophys. Acta* **1784**, 48–55
- Bogoyevitch, M. A., Ngoei, K. R., Zhao, T. T., Yeap, Y. Y. and Ng, D. C. (2010) c-Jun N-terminal kinase (JNK) signaling: recent advances and challenges. *Biochim. Biophys. Acta* **1804**, 463–475
- Bogoyevitch, M. A. (2006) The isoform-specific functions of the c-Jun N-terminal kinases (JNKs): differences revealed by gene targeting. *BioEssays* **28**, 923–934
- Sabio, G. and Davis, R. J. (2010) cJun NH(2)-terminal kinase 1 (JNK1): roles in metabolic regulation of insulin resistance. *Trends Biochem. Sci.* **35**, 490–496
- Borsello, T. and Forloni, G. (2007) JNK signalling: a possible target to prevent neurodegeneration. *Curr. Pharm. Des.* **13**, 1875–1886
- Siddiqui, M. A. and Reddy, P. A. (2010) Small molecule JNK (c-Jun N-terminal kinase) inhibitors. *J. Med. Chem.* **53**, 3005–3012
- Bain, J., McLachlan, H., Elliott, M. and Cohen, P. (2003) The specificities of protein kinase inhibitors: an update. *Biochem. J.* **371**, 199–204
- Fabian, M. A., Biggs, W. H., Treiber, D. K., Atteridge, C. E., Azimioara, M. D., Benedetti, M. G., Carter, T. A., Ciceri, P., Edeen, P. T., Floyd, M. et al. (2005) A small molecule-kinase interaction map for clinical kinase inhibitors. *Nat. Biotechnol.* **23**, 329–336

-
- 41 Barr, R. K., Boehm, I., Attwood, P. V., Watt, P. M. and Bogoyevitch, M. A. (2004) The critical features and the mechanism of inhibition of a kinase interaction motif-based peptide inhibitor of JNK. *J. Biol. Chem.* **279**, 36327–36338
- 42 Barr, R. K., Hopkins, R. M., Watt, P. M. and Bogoyevitch, M. A. (2004) Reverse two-hybrid screening identifies residues of JNK required for interaction with the kinase interaction motif of JNK-interacting protein-1. *J. Biol. Chem.* **279**, 43178–43189
- 43 Podkova, M., Zhao, X., Chow, C. W., Coffey, E. T., Davis, R. J. and Attisano, L. (2010) Microtubule stabilization by bone morphogenetic protein receptor-mediated scaffolding of c-Jun N-terminal kinase promotes dendrite formation. *Mol. Cell. Biol.* **30**, 2241–2250
- 44 Niu, L., Chang, K. C., Wilson, S., Tran, P., Zuo, F. and Swinney, D. C. (2007) Kinetic characterization of human JNK2 α 2 reaction mechanism using substrate competitive inhibitors. *Biochemistry* **46**, 4775–4784
- 45 Ember, B. and LoGrasso, P. (2008) Mechanistic characterization for c-jun-N-terminal kinase 1 α 1. *Arch. Biochem. Biophys.* **477**, 324–329
- 46 Ember, B., Kamenecka, T. and LoGrasso, P. (2008) Kinetic mechanism and inhibitor characterization for c-jun-N-terminal kinase 3 α 1. *Biochemistry* **47**, 3076–3084
- 47 Bonny, C., Oberson, A., Negri, S., Sauser, C. and Schorderet, D. F. (2001) Cell-permeable inhibitors of JNK: novel blockers of β -cell death. *Diabetes* **50**, 77–82
- 48 Chène, P. (2008) Challenges in design of biochemical assays for the identification of small molecules to target multiple conformations of protein kinases. *Drug Discovery Today* **13**, 522–529
- 49 Akritopoulou-Zanze, I. and Hajduk, P. J. (2009) Kinase-targeted libraries: the design and synthesis of novel, potent, and selective kinase inhibitors. *Drug Discovery Today* **14**, 291–297

Received 10 August 2010/16 December 2010; accepted 17 December 2010

Published as BJ Immediate Publication 17 December 2010, doi:10.1042/BJ20101244

SUPPLEMENTARY ONLINE DATA

Characterization of a novel JNK (c-Jun N-terminal kinase) inhibitory peptide

Kevin R. W. NGOEI*, Bruno CATIMEL†, Nicole CHURCH†, Daisy S. LIO*, Con DOGOVSKI*, Matthew A. PERUGINI*, Paul M. WATT‡, Heung-Chin CHENG*, Dominic C. H. NG* and Marie A. BOGOYEVITCH*¹

*Department of Biochemistry and Molecular Biology, Bio21 Molecular Science and Biotechnology Institute, University of Melbourne, Parkville, Victoria 3010, Australia,

†Ludwig Institute for Cancer Research, Parkville, Victoria 3010, Australia, and ‡Phylogica Ltd, Subiaco, Western Australia 6008, Australia

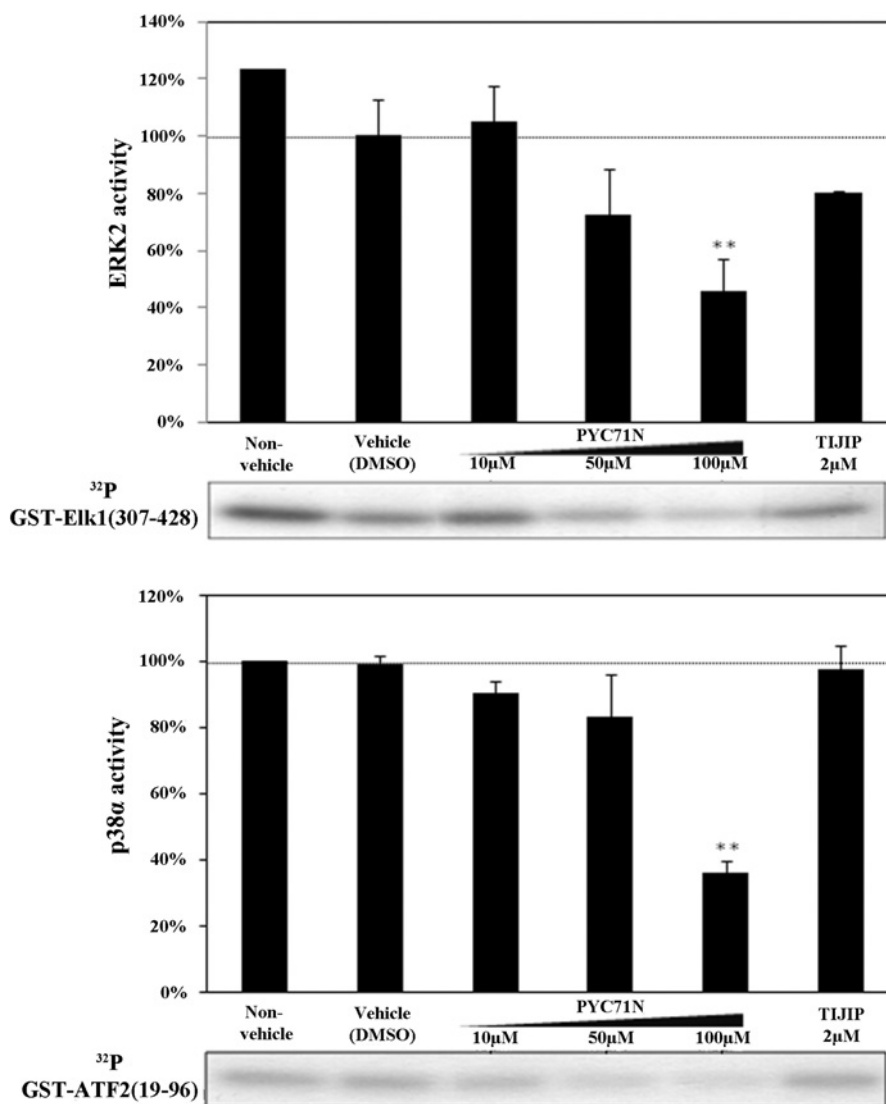


Figure S1 Effects of high concentrations of PYC71N on ERK and p38 activity *in vitro*

Active ERK2 and GST-Erk1 (A) or active p38α and GST-ATF2(19–96) (B) were pre-incubated (5 min, 30°C) with 10, 50 and 100 μM PYC71N before assaying the kinase activity. Incubations in the presence of DMSO at a final concentration 10% (equivalent to the levels included for the assays in the presence of 100 μM peptide) were included as vehicle controls. For each set of results, autoradiography indicated the level of phosphorylation of each substrate (lower panels), and the incorporation of ³²P into each substrate was quantitated by liquid scintillation counting (upper panels). Results were expressed as a percentage of the uninhibited kinase activity in three independent experiments, where error bars represent the S.E.M. and asterisks indicate values statistically significantly different (** $P \leq 0.05$, $n = 3$) from the non-inhibited control reaction.

¹ To whom correspondence should be addressed (email marieb@unimelb.edu.au).

Table S1 Calculated secondary structure of PYC71 and PYC71N

	CDPro database	α -Helix %	β -Strand %	Turn %	Unordered %	RMSD
PYC71	SP22X	25.2	13.0	15.7	46.1	0.069
PYC71 + 30 % TFE	SP29	19.7	32.6	23.0	24.7	0.094
PYC71N	SP37A	0	24.4	14.1	61.5	0.058
PYC71N + 30 % TFE	SMP56	7.9	39.9	22.4	29.8	0.059

Table S2 Native molecular mass of PYC71 and PYC71N peptides

	M_r (kDa)*	M' (kDa)†	RMSD
PYC71	2.71	2.51	0.006
PYC71N	1.81	1.54	0.007

*Relative molecular mass calculated from the amino acid sequence.

†Apparent molar mass calculated from the non-linear least squares best fit to sedimentation equilibrium data (Figure 1C of the main text).

Table S3 Sequences of PYC71N variant peptides

Peptide name	Peptide sequence	Peptide size (amino acid number)	>50% JNK inhibition <i>in vitro</i>
Alanine scan replacement series (Figure 6A of the main text)			
PYC71N	FFWRLNKIFYFID	13	✓
F1→A	AFWRLNKIFYFID	13	✓
F2→A	FAWRLNKIFYFID	13	✓
W3→A	FFARLNKIFYFID	13	✓
R4→A	FFWALNKIFYFID	13	✓
L5→A	FFWRANKIFYFID	13	✓
N6→A	FFWRLAKIFYFID	13	✓
K7→A	FFWRLNAIFYFID	13	✓
I8→A	FFWRLNKAFYFID	13	✓
F9→A	FFWRLNKIAYFID	13	X
Y10→A	FFWRLNKIFAFID	13	✓
F11→A	FFWRLNKIFYAID	13	X
I12→A	FFWRLNKIFYFAD	13	✓
D13→A	FFWRLNKIFYFIA	13	✓
Truncation series (Figure 6B of the main text)			
PYC71N	FFWRLNKIFYFID	13	✓
-1N	FWRLNKIFYFID	12	✓
-2N	WRLNKIFYFID	11	✓
-3N	RLNKIFYFID	10	✓
-4N	LNKIFYFID	9	✓
-5N	NKIFYFID	8	X
-6N	KIFYFID	7	X
-1C	FFWRLNKIFYFI	12	✓
-2C	FFWRLNKIFYF	11	✓
-3C	FFWRLNKIFY	10	X
-4C	FFWRLNKIF	9	X
-5C	FFWRLNKI	8	X
-6C	FFWRLNK	7	X
-1NC	FWRLNKIFYFI	11	X
-2NC	WRLNKIFYF	9	X
Substitutions at positions 4, 5, 7, 9 and 10 (Figure 6C of the main text)			
PYC71N	FFWRLNKIFYFID	13	✓
R4→G	FFWGLNKIFYFID	13	✓
L5→G	FFWRGNKIFYFID	13	✓
K7→G	FFWRLNGIFYFID	13	✓
F9→G	FFWRLNKIGYFID	13	X
Y10→G	FFWRLNKIFGFID	13	X
R4→P	FFWPLNKIFYFID	13	✓
L5→P	FFWRPNKIFYFID	13	✓
K7→P	FFWRLNPIFYFID	13	✓
F9→P	FFWRLNKIPYFID	13	X
Y10→P	FFWRLNKIFPFID	13	X
R4→F	FFWFLNKIFYFID	13	✓
L5→F	FFWRFNKIFYFID	13	✓
K7→F	FFWRLNFIIFYFID	13	✓
Y10→F	FFWRLNKIFFID	13	✓

Received 10 August 2010/16 December 2010; accepted 17 December 2010
 Published as BJ Immediate Publication 17 December 2010, doi:10.1042/BJ20101244